

Lawrence Berkeley National Laboratory

LBL Publications

Title

Experimental Evolution of Extreme Resistance to Ionizing Radiation in Escherichia coli after 50 Cycles of Selection

Permalink

<https://escholarship.org/uc/item/0mt359p5>

Journal

Journal of Bacteriology, 201(8)

ISSN

0021-9193

Authors

Bruckbauer, Steven T
Trimarco, Joseph D
Martin, Joel
[et al.](#)

Publication Date

2019-04-15

DOI

10.1128/jb.00784-18

Peer reviewed

1 **Experimental evolution of extreme resistance to**
2 **ionizing radiation in *Escherichia coli* after 50 cycles of**
3 **selection**

4 **Running title: Directed Evolution of Resistance to Ionizing Radiation**

5 Steven T. Bruckbauer¹, Joseph D. Trimarco^{1,2}, Joel Martin³, Brian Bushnell³, Katherine A.
6 Senn⁴, Wendy Schackwitz³, Anna Lipzen³, Matthew Blow³, Elizabeth A. Wood¹, Wesley S.
7 Culberson^{5,6}, Christa Pennacchio³, and Michael M. Cox^{1#}

8
9 ¹ *Department of Biochemistry, University of Wisconsin – Madison. Madison, WI 53706-1544,*

10 ² *Present address: Duke Microbiology and Molecular Genetics, Duke University School of*
11 *Medicine. Durham, NC 27710,*

12 ³ *DOE Joint Genome Institute - 2800 Mitchell Drive Walnut Creek, CA 94598,*

13 ⁴ *Department of Biomolecular Chemistry, University of Wisconsin – Madison. Madison, WI*
14 *53706-1544,*

15 ⁵ *Department of Medical Physics, School of Medicine and Public Health, University of Wisconsin*
16 *– Madison. Madison, WI 53705-2275,*

17 ⁶ *Department of Medical Physics, University of Wisconsin – Madison. Madison, WI 53705-2275.*

18
19
20
21 #Corresponding author: E-mail: cox@biochem.wisc.edu

22 **Abstract**

23 In previous work (1, 2), we demonstrated that *Escherichia coli* could acquire substantial levels of
24 resistance to ionizing radiation (IR) via directed evolution. Major phenotypic contributions
25 involved adaptation of organic systems for DNA repair. We have now undertaken an extended
26 effort to generate *Escherichia coli* populations that are as resistant to IR as *Deinococcus*
27 *radiodurans*. After an initial 50 cycles of selection using high-energy electron beam IR, four
28 replicate populations exhibit major increases in IR resistance, but have not yet reached IR
29 resistance equivalent to *D. radiodurans*. Regular deep sequencing reveals complex evolutionary
30 patterns with abundant clonal interference. Prominent IR resistance mechanisms involve novel
31 adaptations to DNA repair systems, and alterations in RNA polymerase. Adaptation is highly
32 specialized to resist IR exposure, as isolates from the evolved populations exhibit highly variable
33 patterns of resistance to other forms of DNA damage. Sequenced isolates from the populations
34 possess between 184 and 280 mutations. IR resistance in one isolate, IR9-50-1, is derived largely
35 from four novel mutations affecting DNA and RNA metabolism: RecD A90E, RecN K429Q,
36 and RpoB S72N/RpoC K1172I. Additional mechanisms of IR resistance are evident.

37

38 **Importance**

39 Some bacterial species exhibit astonishing resistance to ionizing radiation, with *Deinococcus*
40 *radiodurans* being the archetype. As natural IR sources rarely exceed mGy levels, the capacity of
41 *Deinococcus* to survive 5,000 Gy has been attributed to desiccation resistance. To understand the
42 molecular basis of true extreme IR resistance, we are using experimental evolution to generate
43 strains of *Escherichia coli* with IR resistance levels comparable to *Deinococcus*. Experimental
44 evolution has previously generated moderate radioresistance for multiple bacterial species.

45 However, these efforts could not take advantage of modern genomic sequencing technologies. In
46 this report, we examine four replicate bacterial populations after 50 selection cycles. Genomic
47 sequencing allows us to follow the genesis of mutations in populations throughout selection.
48 Novel mutations affecting genes encoding DNA repair proteins and RNA polymerase enhance
49 radioresistance. However, more contributors are apparent.

50

51 **Introduction**

52 Ionizing radiation (IR) can damage any cellular component, either through direct ionization by
53 high energy photons and electrons, or indirect ionization from reactive oxygen species (ROS)
54 produced by radiolysis of water molecules. Fortunately, levels of IR sufficient to cause
55 widespread oxidation of proteins or extensive DNA damage (including double strand breaks) are
56 rarely encountered in the environment. Surprisingly, a number of microbial species and a few
57 multicellular organisms have evolved extreme resistance to IR (3, 4). The bacterium
58 *Deinococcus radiodurans* is the first-discovered and remains the best-studied example of this
59 extremophile phenotype. *D. radiodurans* survives exposure to 5,000 Gray (Gy) of IR with no
60 lethality, 1000-times the lethal dose for a human. In the case of this bacterium, extreme IR
61 resistance appears to be a byproduct of natural selection for desiccation tolerance (5-7). *D.*
62 *radiodurans* is not alone. Organisms with high levels of IR resistance can be found readily,
63 particularly in arid environments (8, 9).

64 IR resistance in *D. radiodurans* has been attributed in large measure to an enhanced
65 capacity to ameliorate ROS produced by IR using a variety small molecules and metabolites (10-
66 12). *D. radiodurans* possesses a fairly standard complement of DNA repair systems. However,
67 specialized adaptations of those systems and the evolution of a few novel DNA metabolic

68 functions may contribute substantially to the extraordinary capacity of *D. radiodurans* to repair
69 an extensively damaged genome (13-15).

70 Substantial increases to bacterial IR resistance can be generated in the laboratory by
71 directed evolution (16-19). The advent of advanced DNA sequencing technologies that reveal
72 genomic changes in populations has revolutionized studies of molecular evolution. Mutational
73 trajectories associated with adaptation have been defined in bacteria (20-26), viruses (27-31),
74 yeast (32, 33), and mammalian tumors (34-45). These studies have greatly enhanced the
75 experimental foundation of many phenomena predicted by evolutionary biology, including
76 clonal interference (22, 24, 33), diminishing returns epistasis (20, 46), and genetic parallelism
77 (21-24, 26, 29).

78 We have utilized directed evolution as a tool providing a facile path to a better
79 understanding of mechanisms underlying the extreme IR resistance phenotype in bacteria. We
80 previously exposed four replicate populations of *Escherichia coli* to 20 iterative rounds of
81 gamma-ray IR and observed significant increases in IR resistance (1). Focusing on isolates from
82 each population, we determined that IR resistance arose from enhanced DNA repair (reflected in
83 mutant alleles of the recombinase RecA, replicative helicase DnaB, putative helicase YfjK, and
84 replication restart machinery), and changes in the regulation of central metabolism and cellular
85 responses to oxidative damage (through an allele of the anaerobic metabolism transcription
86 factor, FNR) (1, 2, 47).

87 The overall IR resistance of these populations, while increased substantially, did not
88 reach a level comparable to *D. radiodurans*. Efforts to further enhance the IR resistance
89 phenotype have been constrained both by source decay (altering irradiation dose rate parameters
90 and increasing times required to impose a particular dose on a sample) and by new governmental

91 policies mandating a general decommissioning of radioactive sources used for research. To
92 generate *D. radiodurans*-like levels of IR resistance in evolved *E. coli*, we have embarked on a
93 new and more ambitious effort with four new populations. This new effort employs a clinical
94 linear accelerator (Linac) of a type utilized for radiation treatment of cancer patients. Using this
95 device to produce a high energy electron beam, we can achieve a dose rate of 72 Gy/min, nearly
96 4-fold higher than that used in the previous directed evolution study (1, 2). Use of this instrument
97 eliminates the problem of radioactive source decay and greatly reduces the amount of time
98 required for exposure to kGy levels of IR. The higher dose rate also allows us to explore
99 adaptation to a potentially much more challenging IR environment than that utilized in earlier
100 trials. We can also begin to assess the effect of dose rate on an evolution trial.

101 In this report, we characterize the four new *E. coli* lineages (IR9, IR10, IR11, and IR12)
102 after the first 50 rounds of selection (IR9-50, IR10-50, IR11-50, and IR12-50). The dose required
103 to kill 99% of the cells in each population has increased from approximately 750 Gy to over
104 2000 Gy. These populations are highly resistant compared to the previously evolved isolates
105 CB2000 and CB3000 (1, 2), which appear to be poorly adapted to the higher dose rates applied
106 with the electron beam IR. Deep genomic sequencing of populations after every other selection
107 cycle allow us to explore the full breadth of mutations and provides a revealing window on the
108 evolution of IR resistance. To unveil IR resistance mechanisms, we focus on the genetic
109 parallelism between the four lineages, as reflected in a representative isolate from population
110 IR9-50, IR9-50-1. The results both reinforce some earlier conclusions and offer new insights.
111 The phenotype in IR9-50-1 is largely explained by four mutations, none of which appeared in
112 our previously evolved *E. coli* populations. Although adaptations in DNA repair machinery are
113 again prominent, but now feature novel mutations in *recD* and *recN* which enhance IR

114 resistance. Furthermore, alterations in RNA polymerase (primarily variants in genes *rpoB* and
115 *rpoC*) also contribute substantially to an IR resistant phenotype. The other three evolved
116 populations exhibit patterns that both reinforce those seen in IR9-50 but also suggest direct
117 competition of two distinct pathways of evolved IR resistance (through either paired mutations
118 of the *recA* and *recD* genes, or a grouping of *rpoB/C*, *recD*, and *recN*). Further adaptation to IR
119 (beyond the mutations described herein) has occurred in each of the four populations, and
120 remains to be explored.

121

122 **Results**

123 **High-energy electron beam IR kills *E. coli* at a similar rate to high-energy photon IR**

124 In this new set of evolution trials, we utilized a Linac to deliver doses with a high energy
125 electron beam. Our previous evolution trials to generate IR resistant *E. coli* utilized a ⁶⁰Co source
126 with a dose rate of approximately 19 Gy/min (1). Using the Linac in electron mode, we were
127 able to deliver the same doses at 72 Gy/min. As there is no source decay with this device, the
128 dose rate will remain constant over the years required for an extended evolution trial. The dose
129 delivered by the Linac was verified using thermoluminescent dosimeters (TLDs). The delivered
130 dose varied by less than 5% of the calculated dose (Table S1).

131 Although the Linac electron beam and photon sources are different, the dose delivery
132 mechanisms are very similar. In order to rule out any differences between electron and photon
133 modes, we sought to determine if high-energy electron beam ionizing radiation (IR) kills *E. coli*
134 similarly to high-energy photon IR. We note that the ⁶⁰Co and ¹³⁷Cs sources used in our previous
135 directed evolution studies (1, 2, 47) produced high-energy photons. The Linac used in this study
136 has both an electron and photon mode. By changing the distance of the *E. coli* cultures to the

137 source of the IR beam, the Gray per minute (Gy/min) dose rate can be made equivalent between
138 these modes. At a dose rate of 17 Gy/min, high energy electrons and photons killed nearly an
139 identical percentage of *E. coli* MG1655 culture at 1000 Gy, with the electron beam being slightly
140 more potent (Fig. 1). Therefore, the two IR modes appear to have comparable effects at the level
141 of bacterial survival.

142

143 **Directed evolution of extreme IR resistance over 50 rounds of selection**

144 Beginning with a single culture of the *E. coli* strain MG1655 split into four, we generated
145 four IR resistant populations using a modified version of a previously established directed
146 evolution protocol (1) as described in the Materials and Methods and depicted in Fig. 2A.

147 Using this protocol, we carried out 50 iterative cycles (with selection cycles occurring
148 approximately once per week). The resulting populations were designated IR9-50, IR10-50,
149 IR11-50, and IR12-50 (Fig. 2B). Over these rounds of evolution, the dose required to kill 99% of
150 each culture increased from approximately 750 to 2300 – 2500 Gy (Fig. 3A). At round 50, these
151 populations were highly radioresistant compared to the parent MG1655 strain (Fig. 3B).
152 Previously described IR resistant *E. coli* isolates (1, 2, 47), which were evolved to withstand
153 ⁶⁰Co IR at about 4-fold lower dose rates, were only moderately more resistant to the beam
154 generated by the Linac compared to the parent strain and were greatly surpassed by the
155 populations generated in this study (Fig. 3B). Populations IR9-50, IR10-50, IR11-50, and IR12-
156 50 have not yet reached the level of IR resistance of the bacterium *Deinococcus radiodurans* but
157 have made significant progress towards this goal. We note that *D. radiodurans* was significantly
158 more sensitive to the higher dose rate in the Linac electron source than it was to the lower dose
159 rates in the ⁶⁰Co photon source (Fig. 3B) (4, 11, 13).

160
161
162
163
164
165
166
167
168
169
170
171
172
173
174
175
176
177
178
179
180
181
182

Growth phenotypes of evolved population isolates

The IR resistance phenotype of these experimentally-evolved populations was not accompanied by an apparent growth defect in LB rich medium. An isolate from each population at round 50 of selection (IR9-50-1, IR10-50-1, IR11-50-1, and IR12-50-1) produced growth curves comparable to the parent MG1655 strain in LB (Fig. 4A). However, growth defects of these isolates became apparent when inoculated in other growth media. In a defined rich medium supplemented with glucose, EZ medium, isolate IR12-50-1 failed to grow and isolates IR9-50-1 and IR11-50-1 exhibited growth defects easily observed in a standard growth curve (Fig. 4B). The isolate IR10-50-1 grew similarly to MG1655 in EZ medium and was the only of the four isolates to grow in M9 minimal medium supplemented with glucose (Fig. 4C). Although IR9-50-1, IR11-50-1, and IR12-50-1 have potentially inactivating mutations in key amino acid biosynthetic pathways that could prevent growth in minimal medium (IR10-50-1 does not have a mutation which would clearly affect amino acid biosynthesis), supplementing minimal medium with these amino acids did not rescue the ability of these isolates to grow (Fig. S1).

Highly sensitive growth competition assays (48) in LB medium can reveal subtle growth phenotypes of these isolates that are not readily apparent when comparing standard growth curves (Fig. 5). When paired with the parent wild type *E. coli* strain in a mixed culture of LB, all four evolved isolates were rapidly outcompeted, even with significant dilutions to bias the starting culture ratios towards the evolved strains. These results indicated that 50 rounds of selection in this directed evolution protocol came with an underlying fitness cost, even when selection is not being applied.

183 **Evolved isolates exhibit variable resistance to non-IR DNA damaging agents**

184 Isolates from the four evolved populations after 50 cycles of selection revealed that
185 resistance to IR does not correlate in any predictable way with resistance to other DNA
186 damaging agents, even within a single population (Fig. 6 and 7). Multiple isolates from each
187 population exhibited highly variable levels of resistance to UV radiation (Fig. 6), mitomycin C
188 (which causes DNA intrastrand crosslinks), ciprofloxacin (which causes DNA double-strand
189 breaks through inhibition of DNA gyrase), bleomycin (which causes DNA double-strand breaks
190 and apurinic/apyrimidinic sites through a ROS mediated mechanism (49, 50)), and hydroxyurea
191 (which has a complex mechanism of action that both reduces dNTP production and causes ROS-
192 mediated DNA damage) (51-54)(Fig. 7). While some isolates exhibited increased resistance to
193 these DNA-damaging agents, others showed no change or increased sensitivity. The results
194 indicate that the directed evolution trials are generating specialists that are uniquely adapted to
195 IR resistance.

196

197 **Deep-sequencing reveals unique evolutionary histories of the evolved populations**

198 We utilized deep-sequencing technology to monitor genomic changes as IR resistance increased
199 with continued selection cycles. At every other round of selection, genomic DNA was prepared
200 from each population and submitted to the Joint Genome Institute (Walnut Creek, CA) for
201 sequencing to determine all mutations present in each population. Stitching together these
202 snapshots revealed the underlying complexity of these evolving populations (Fig. 8A-D).
203 Depicted in Fig. 8 are the allele frequencies of all mutations detected above 2% frequency at
204 each even round of selection for each lineage. Each line represents a single mutation; groups of
205 mutations that rise and fall in frequency together are inferred to be linked within a sub-

206 population. The number of sub-populations and total number of mutations increased rapidly (Fig.
207 8E). The steady accumulation of mutations over time suggests that mutator strains have not yet
208 appeared in these populations. The complete dataset upon which Fig. 8 is based is provided in
209 Supplementary Data 1 through 4.

210 Despite starting from the same parent strain, the evolutionary path of each population was
211 unique. The only event in common to each population was the excision of the e14 prophage, as
212 indicated by four mutations in the *icd* gene in which the prophage is inserted (as depicted by the
213 initial single black line appearing in each population in Fig. 8A-D). When e14 is excised, the *icd*
214 gene is restored to the wild-type sequence. Despite excision of e14 occurring quickly in each
215 population, that excision became fixed in only three of them. In the IR10 lineage, the sub-
216 population that lost the e14 prophage was driven extinct by another sub-population and e14 is
217 retained in population IR10-50.

218 Each lineage experienced significant clonal interference, as depicted by the numerous
219 competing sub-populations in Fig. 8A-D. Competition of sub-populations within lineages IR11
220 and IR12 significantly reduced the rate of fixation events in each lineage. In IR11 (Fig. 8C), no
221 mutations were able to fix from approximately round 16 to round 50 of selection due to severe
222 clonal interference. In IR12 (Fig. 8D), no subpopulation was able to sweep to fixation until 30
223 cycles of selection were completed. Although clonal interference is apparent in lineages IR9 and
224 IR10, its effects are far less severe than in IR11 and IR12. In IR9 (Fig. 8A), no subpopulation
225 was able to fix post-e14 phage excision until approximately round 20. After this event, another
226 subpopulation swept to fixation unimpeded (defined as a continuous, linear rate of increasing
227 allele frequency). A final subpopulation was able to eventually reach 100% frequency, but was in
228 competition with a separate subpopulation for approximately 12 rounds of selection.

229 Surprisingly, lineage IR10 (Fig. 8B) has approximately 6 distinct subpopulations which swept to
230 fixation, and each was not noticeably affected by intra-population competition. The differing
231 trajectories of evolution in each population may reflect the relative fitness of the mechanisms of
232 IR resistance employed by each eventual successful subpopulation.

233 At round 50 of selection, there were distinct differences in the amounts and types of
234 mutations between populations. Populations IR9-50 and IR10-50 are the most homogenous, with
235 approximately 16 and 17%, respectively, of the total high confidence (> 2% allele frequency)
236 mutations being fixed (detected at > 99% frequency). In contrast, only 4% and 11% of high
237 confidence mutations in IR11-50 and IR12-50 are fixed, respectively (Table 1). Although IR9-50
238 and IR10-50 shared a similar percentage of fixed mutations, IR9-50 and IR12-50 had the highest
239 total number of mutations. Each population had a ratio of non-synonymous to synonymous
240 mutations greater than two.

241 GC to AT and AT to GC transitions were detected in high numbers, agreeing with
242 mutational patterns detected in previously evolved IR-resistant *E. coli* populations (1, 2). Base
243 substitutions are approximately 50% transitions and 50% transversions, whereas *E. coli* exposed
244 to ⁶⁰Co gamma-ray irradiation exhibit transversions at about four times the frequency of
245 transitions (1, 55). In particular, GC to TA transitions appeared at very high levels in each
246 population, indicative of significant template-strand 8-oxodG-mediated mutagenesis (56). These
247 results indicated that the selection utilized in the current study produces a substantially different
248 mutational, and perhaps DNA damage, spectrum relative to the populations evolved to resist
249 ⁶⁰Co-produced IR.

250

251 **Mutations which enhance IR resistance in isolate IR9-50-1**

252 We have begun characterization of evolved IR resistance after 50 cycles of selection. To
253 define mutations that made significant contributions to the phenotype, we counted on a
254 substantial degree of genetic parallelism (21, 22, 26) between the four populations. We focused
255 on mutations meeting the following criteria: i) the mutations were non-synonymous; ii)
256 mutations occurred in a gene that was mutated in at least two additional populations; iii)
257 mutations in the gene achieved at least 10% abundance at some point during selection in each
258 population in which they appeared; and iv) the mutation remained in the population at round 50
259 of selection. These criteria narrowed the search to mutations appearing in six genes, including
260 those involved in recombinational DNA repair (*dinI*, *recD*, and *recN*), transcription (*rpoB*),
261 regulation of anaerobic metabolism (*arcB*), and copper ion transport (*copA*). Two additional gene
262 alterations were analyzed: Nth C203Y and RecA A290S. These did not meet the criteria we set
263 in the current study but were the only two variants, aside from the loss of the e14 prophage,
264 where the exact same mutation appeared in two populations. The RecA A290S variant, which is
265 fixed in population IR10-50 and also appears in the IR11 lineage, is the only variant detected in
266 this current study that was also detected in an earlier study (1). The relevant variants are listed in
267 Table 2.

268 To determine the molecular basis of IR resistance in one of the populations, we more
269 carefully characterized one isolate from population IR9-50: IR9-50-1. IR9-50-1 contained over
270 300 mutations (Table 3). A complete dataset for mutations found within the sequenced isolates is
271 presented in Supplementary Data 1 through 5, with isolate data in the appropriate lineage data
272 file.

273 IR9-50-1 is representative of several mutational patterns seen in most of the populations,
274 as it has mutations in *dinI*, *recD*, *recN*, *rpoB*, *rpoC*, and *copA* (which contain the majority of

275 mutations listed in Table 2). This isolate does not have mutations in *arcB*, *nth*, and *recA*.
276 However, a mutation in *arcB*, leading to the variant gene product ArcB N405D, did appear
277 earlier in the IR9 lineage but was driven to extinction via clonal interference. As such, five
278 protein variants present in IR9-50-1 were investigated for contributions to IR resistance: RecD
279 A90E, RecN K429Q, DinI R28H, RpoB S72N, and CopA V270F. The ArcB N405D mutation
280 was also examined as it represented a mutational pattern in other populations. A mutation in
281 *rpoC* (which codes for the K1172I variant) was also included in the strains with RpoB S72N, as
282 the genomic proximity of *rpoC* to *rpoB* did not allow for ready separation of these two mutations
283 with the methods used here.

284 To assess the potential contribution of mutations identified in this way to IR resistance,
285 we first isolated each mutation in an otherwise wild-type genetic background. We then took the
286 evolved isolate and converted the mutation being studied to wild-type in the otherwise mutant
287 background to determine if it caused phenotypic loss. We moved these mutations singly and in
288 combination into a derivative of the parent *E. coli* strain (MG1655) lacking the ϕ 14 prophage (as
289 this prophage appears to excise from the chromosome after IR exposure and each subsequent
290 mutation occurred in this genetic background (1, 2)). This strain, Founder $\Delta\phi$ 14 (1, 2), thus
291 provided the otherwise wild-type genetic background to determine the contribution of each
292 mutation to IR resistance. We determined that the RecD A90E and RpoB S72N/RpoC K1172I
293 variants each provided a significant increase in IR resistance (Fig. 9A) when isolated in this
294 otherwise wild type background. A combination of these two alleles did not significantly
295 increase IR resistance of the parent strain beyond either individual mutation, indicating that they
296 do not contribute additively. The effects of these two alleles were confirmed by converting each
297 of them singly and in combinations to the wild-type allele in the IR9-50-1 genetic background

298 (Fig. 9B). Interestingly, the RecN K429Q mutation did not significantly alter IR resistance of
299 Founder $\Delta e14$. However, when this variant was converted to the wild-type RecN in the IR9-50-1
300 genetic background, IR resistance was dramatically lowered. When these four mutations were
301 eliminated from a derivative of IR9-50-1 that retained the other 308 mutations, IR resistance was
302 not reduced lower than the wild-type RecN single mutant, suggesting a key role for the RecN
303 K429Q variant.

304 The RecD A90E mutation appeared to be at least a partial loss of function, as deleting the
305 *recD* gene from Founder $\Delta e14$ increased IR resistance just as much as the RecD A90E variant
306 (Fig. 9A). These data agree with the fact that a truncated, and likely inactive, RecD variant
307 appeared earlier in the IR9 lineage and in the IR10 lineage (Table 2). The DinI, CopA, and ArcB
308 variants did not contribute significantly to IR resistance when isolated in the wild type
309 background; additionally, converting the *dinI* or *copA* genes to the wild-type sequence in IR9-50-
310 1 did not increase IR sensitivity of this strain.

311 Following the allele frequency of mutations in genes that demonstrably contributed to IR
312 resistance (*recA*, *recD*, *recN*, and *rpoB*), a new pattern emerged (Fig. 10). In the lineages IR9,
313 IR11, and IR12 there was a conserved temporal order in the appearance of mutations. First, the
314 $e14$ prophage was lost, followed by an *rpoB* mutation and then a *recD* mutation along with a
315 *recN* mutation. In the IR12 lineage, the primary *rpoB* mutation was a synonymous coding
316 mutation. However, this did not negate a possible effect of this mutation, potentially at the level
317 of codon usage (RpoB D1203, GAC (WT) to GAT (mutant): 0.37 to 0.63 frequency). The trend
318 was clear in lineages IR9 and IR11, where all the mutations were non-synonymous. IR10 was the
319 only lineage that did not conform to this trend. Although the $e14$ prophage did excise in lineage
320 IR10, the sub-population that lost the prophage was outcompeted by another that maintained the

321 prophage and contained a variant of both RecD (N124D) and RecA (A290S). This RecA variant,
322 A290S, was previously observed in *E. coli* populations evolved to resist IR (1, 2) and also
323 significantly contributes to electron beam IR resistance (Fig. S2). This is the only mutation
324 observed in these four populations that appeared in the previously evolved *E. coli* populations,
325 aside from loss of the e14 prophage (1, 2). After the appearance of the RecA A290S and RecD
326 N124D variants, no RpoB variants appeared in the IR10 lineage until nearly round 40 of
327 selection, and those variants (F15L and K1200E) had not yet reached even 50% frequency in
328 IR10 at round 50. It appears that the evolutionary path observed in IR10 nearly occurred in
329 population IR12 as well, where the sub-population that lost the e14 prophage was almost
330 outcompeted by a different lineage (the competing sub-population again featuring RecD
331 (T568A) and RecA variants (E19K)), before being carried to fixation with the apparent help of a
332 different RecD variant (S92I). A sub-population with a RecD (W534R) and RecA variant
333 (E286G) also reached high frequency in IR11 but was slowly outcompeted by a subpopulation
334 with a different RecD variant (A550E) after it gained a second RpoB variant (P535L). In all of
335 these populations, after either RpoB/RecD/RecN or RecA/RecD variants fixed, the opposing
336 grouping of mutations did not appear within the given population. These results imply that these
337 two evolutionary pathways confer competing yet overlapping mechanisms of IR resistance.

338

339 **Prominent mutations can contribute to enhanced growth phenotypes**

340 If variants of proteins such as ArcB, CopA, and DinI do not contribute to IR resistance,
341 do they make some other contribution to fitness that explains their prominence? We have
342 previously observed that high frequency mutations in experimentally evolved populations may
343 contribute to enhanced growth rates, rather than IR resistance (47). Part of the selection protocol

344 involves an outgrowth step, after irradiation, in which mutants that grow slowly could be lost.
345 Consistently, the ArcB N405D mutation significantly enhanced the growth phenotype of
346 Founder $\Delta e14$ in a growth competition assay relative to the same strain with a wild-type ArcB
347 (Fig. 11). The DinI R28H and the CopA V270F mutations had no measurable effect on growth
348 (Fig. S3). Mutations that enhance the growth phenotype of these populations are likely
349 important, as evidenced by their inability to grow well in media aside from LB (Fig. 6) and their
350 inability to compete with Founder $\Delta e14$ in mixed culture without IR selection (Fig. 5). In effect,
351 certain mutations may arise that compensate for growth defects conferred by mutations that
352 contribute to IR resistance or deleterious, hitchhiking mutations. Founder $\Delta e14$ with the RpoB
353 S72N and RpoC K1172I variants is outcompeted quickly by Founder $\Delta e14$ with wild-type RNA
354 polymerase (Fig. 11). These results indicate that in order to develop high levels of IR resistance,
355 mutations which buffer against deleterious effects on viability must also rise to prominence in
356 these populations. Although not arising in the same genetic background, the growth phenotype of
357 the ArcB N405D variant indicates that these populations have developed variants which can
358 enhance growth to the degree which mutations such as the RpoB S72N/RpoC K1172I variants
359 impede growth.

360

361 **Discussion**

362 It is clear that latent within the *E. coli* genome is a capacity for resistance to extreme
363 doses of ionizing radiation. After 50 rounds of selection with high-energy electron beam IR, the
364 dose required to kill 99% of each of these four replicate populations increased by over three-fold
365 to approximately 2500 Gy (Fig. 3A). After a dose of 1500 Gy, this translates into an increase in
366 survival of 4-5 orders of magnitude (Fig. 3B). The dose of electron beam IR that these strains

367 can withstand far exceeds that of previously evolved IR-resistant isolates (1, 2) , at least when
368 the new and higher dose rate is applied. These populations vary in their growth phenotypes (Fig.
369 3B and 4) and resistance to other forms of DNA damage (Fig. 6 and 7), indicating that they are
370 specialized to withstand high doses of IR.

371 Most laboratory exercises in experimental evolution have been characterized by a rapid
372 decline in the rate of fitness increase, as fitness approaches some biologically determined
373 optimum for a given agent of selection (22, 57, 58). One key difference between the current
374 experiment and many other long-term directed evolution experiments is that the selection agent
375 here is not a constant. The dose of IR inflicted on the populations increases as resistance levels
376 increase. Increased selection pressure to meet a defined, desired phenotype throughout selection
377 is not a novel protocol (58), yet in our evolution experiment there is no evident deceleration in
378 the rate of fitness gains. Genetic patterns (parallelism) have allowed us to identify some key
379 contributors to the growing IR resistance phenotype. However, the continuing advance of IR
380 resistance and allele diversity in all populations also suggests that the pool of potential adaptive
381 mutations is much greater than that now present in any one population. As selection continues,
382 substantial additional gains in unique pathways may be expected. Ionizing radiation is not only a
383 selection agent, but also a potent mutagen. Although this study was not initiated with the goal of
384 exploring mechanisms of molecular evolution, we anticipate that the datasets provided in
385 Supplemental Data 1 through 4 will be of use to investigators in that field.

386

387 **Modified DNA repair proteins and RNA polymerase enhance IR resistance**

388 Each population has traversed unique evolutionary paths to reach the same goal (Fig. 8A-
389 D). Despite varied levels of clonal interference in each population, significant genetic parallelism

390 in these populations allow us to identify at least some of the contributors to extreme IR
391 resistance. In one isolate from population IR9-50, IR9-50-1, mutations in *recD*, *recN*, and
392 *rpoB/rpoC* increase IR resistance of the Founder $\Delta e14$ parent-derivative. However, these variants
393 – singly or together – do not account entirely for the IR resistance phenotype of IR9-50-1 at a
394 dose of 1000 Gy (Fig. 9A and B). None of these genes have been previously implicated as
395 mutational targets contributing to IR resistance (1, 2, 47).

396 The effects of mutations in these genes reveal complex interactions. When present in an
397 otherwise wild-type background, the mutations in *recD* and *rpoB* exhibit a clear contribution to
398 IR resistance, although results with the *recN* mutation were variable. The *recD* and *rpoB* effects
399 were not additive, and combining them demonstrated diminishing returns epistasis. When the
400 *rpoB* mutation was reverted to wild-type in the IR9-50-1 mutant background, the IR resistance
401 phenotype was reduced little or not at all. However, reverting the *recD* and *recN* mutation to
402 wild-type resulted in a considerable loss of IR resistance. It appears likely that a complete
403 genetic deciphering of the IR resistance of IR9-50-1 and other isolates will require a more
404 systematic consideration of relationships between mutations and genetic backgrounds.

405 Although additional contributions are clearly present, the alterations in RecD, RecN, and
406 RpoB/RpoC (Fig. 9) provide the clearest evidence for phenotypic contributions in the current
407 work. RecD is part of the RecBCD heterotrimer responsible for preparing ssDNA required for
408 RecA loading, initiating homologous recombination. The RecD A90E variant is likely a loss of
409 function mutation, as a RecD deletion in the Founder $\Delta e14$ background increases IR resistance as
410 much as the A90E variant in this background. RecD inactivation produces a hyper-
411 recombination phenotype (59-62). Increased homologous recombination could be of significant

412 use to repair highly fragmented DNA post-IR, with approximately 15 DSBs generated at 1000
413 Gy (3).

414 RecN is a cohesin-like protein which is involved in RecA-mediated double-strand break
415 repair (63-66). There is little known about the precise function of RecN, though it has been
416 implicated in maintaining proximity of broken dsDNA ends to an active RecA filament. The
417 function of the K429Q variant is unknown, but the K429 residue is positioned in a RecN domain
418 highly conserved among bacteria. The K429Q variant is unlikely to be a loss of function, as *recN*
419 deletion greatly enhances IR sensitivity (2, 67). Further work on these RecN variants may shed
420 new light on the function of the RecN protein.

421 RpoB and RpoC are the beta and beta-prime subunits of RNA polymerase, respectively.
422 Stringent mutations of RNAP, which mimic the effects of ppGpp binding and therefore the
423 stringent response, are located primarily in RpoB and RpoC (68). Some of these stringent
424 mutants are capable of rescuing UV-sensitivity of *ruvABC* mutants of *E. coli*, potentially due to
425 decreased stability of contacts of RNAP with DNA (69, 70). Similar to these previous
426 observations, the mutations in RpoB that are prevalent in our evolved populations do not locate
427 to a single region of RpoB and therefore may affect DNA interaction throughout the DNA
428 channel formed by RpoB/RpoC. Previously described stringent mutations L571Q and H1244Q
429 mutants (69, 70) affect residues near those affected in the current study. These mutations likely
430 decrease stability of RNAP on DNA and may allow for easier removal of RNAP that has stalled
431 at a DNA lesion. Removal of stalled RNAP may be crucial for efficient DNA repair due to
432 RNAP occluding the lesion from repair machinery or providing a major obstacle to DNA
433 replication (71). Additionally, many stringent mutants of RNAP also confer resistance to the
434 antibiotic Rifampicin. Mutated variants of RNAP at P535 (72) and S574 (73-75) (which have

435 also been isolated in this study) have previously been isolated using selection for rifampicin
436 resistance. Although these are the first RNA polymerase mutations detected in *E. coli* evolved
437 for IR resistance, similar mutants have been generated during experimental evolution of *E. coli*
438 for trimethoprim and doxycycline resistance (58), heat tolerance (76, 77), growth in nutrient-
439 limited conditions (78, 79), and acid resistance (80, 81). Modifications in RNA polymerase may
440 confer enhanced fitness throughout serial passaging, a common feature of experimental evolution
441 studies. This advantage, combined with a potential ability to enhance DNA repair, may explain
442 the rapid appearance of *rpoB* or *rpoC* alleles in each evolving lineage (except IR10).

443

444 **Excision of the e14 prophage is induced by selection for IR resistance**

445 The only event common to each of the four populations is the excision of the e14
446 prophage, which was evident by round two of selection. However, in lineage IR10 the
447 subpopulation that lost e14 was outcompeted and driven extinct by cycle ten. Despite no
448 apparent mutations within e14 that may prevent its excision, the e14 prophage remains within
449 lineage IR10. It is unclear why e14 excision is the first clear event to happen in each population
450 (an event that also occurred early in evolution of our previously evolved gamma-ray IR-resistant
451 *E. coli* populations (1, 2). Excision of the e14 prophage is predicted to be under regulation of the
452 SOS response, this event may simply be an artifact of the *E. coli* DNA damage response (82).
453 However, the e14 genome does encode two potentially lethal cell division inhibitor proteins: a
454 homologue of the lambda phage protein Kil and SfiC. Loss of these proteins may itself be
455 selective pressure. Indeed, loss of the e14 has been previously noted during experimental
456 evolution (83) Interestingly, deletion of the e14 prophage has also been observed to cause

457 variable resistance to many antimicrobial agents, including increased resistance to hydrogen
458 peroxide (84).

459

460 **Direct competition between two pathways to IR resistance dictates adaptation**

461 Population sequencing also reveals the underlying competition of lineages within each
462 population. Clonal interference is a hallmark of these populations. While much of this study
463 focuses on the current end-point (each population after 50 cycles of selection), observing
464 evolution over the remaining 49 cycles allows us to understand the genetic context in which new
465 mutations arise and how the successful lineages were able to outcompete other fit, but ultimately
466 unsuccessful, lineages. This competition within populations was almost immediately apparent.

467 There is an apparent competition between lineages which contain alleles of *rpoB* and
468 those with *recA* alleles. In the current protocol, with its much higher IR dose rate, *recA* alleles
469 are less common than observed in our earlier study, and novel *rpoB*, *recD*, and *recN* alleles
470 predominate. In IR9, a single *recA* variant appeared (Y294C) but only reached approximately
471 12% frequency in the population before being driven extinct by round 20 of selection. This
472 population successfully lost the e14 prophage and then gained an *rpoB* allele followed by *recD*
473 and *recN* alleles. The appearance of *recD* and *recN* alleles in tandem occurred in three of the four
474 populations, and each contributes similarly to IR-resistance in a wild-type background (Fig. S4).
475 In IR10, the RecA/RecD variant pair appears very early, and rapidly outcompetes the lineage that
476 lost the e14 prophage. After this event, the only mutation that became fixed within the
477 population (of those common to all four populations which we are focusing on) is another RecD
478 variant. RpoB variants do not appear until at least round 40 of selection in IR10, and by round
479 50, these variants do not yet appear to be on a path to fixation. No high-frequency *recN* allele has

480 appeared in IR10. The IR11 and IR12 lineages followed a path similar to that taken by IR9. In
481 the IR11 lineage, loss of the e14 prophage and subsequent gain of an *rpoB* allele became fixed.
482 In this genetic background, two separate sub-populations containing RecN/RecD and
483 RecA/RecD variants, respectively, later reached prominence. The RecN/RecD subpopulation
484 gained a variant of RpoB which assisted in driving this sub-population to fixation and the
485 RecA/RecD to extinction. Finally, IR12 almost began on a similar evolutionary trajectory as
486 IR10. A sub-population that lost the e14 prophage and gained an *rpoB* allele (which leads to a
487 synonymous coding mutation) was nearly outcompeted by a RecA/RecD variant sub-population,
488 before a RecN/RecD variant-pair rescued the sub-population that had lost e14. By round 40 of
489 selection, the winning subpopulation reached fixation.

490 Despite our focus on the genetic parallelism between these four populations, it is evident
491 that each population has begun to develop unique adaptations. Of the total number of fixation
492 events in each lineage (excluding excision of the e14 prophage, IR9: 2; IR10: 5; IR11: 2; IR12:
493 2) tracking mutations in *rpoB/recA/recD/recN* only fully accounts for such events in IR9 and
494 IR11. In all four lineages, major subpopulations that have arisen after fixation of
495 *rpoB/recA/recD/recN* combinations are completely unaccounted for by the criteria used to
496 identify the mutations tested in this study. While it is clear that e14 excision and competition
497 between RecA/RecD and RpoB/RecD/RecN provides a path to enhanced IR resistance, this
498 appears to be only the first step on a complicated fitness landscape. New methods must be
499 applied to determine the unique paths taken by each of the four lineages.

500

501 **Source of IR and dose rate alter the molecular basis for experimentally-evolved IR**
502 **resistance**

503 Populations IR9-50, IR10-50, IR11-50, and IR12-50 provide us with a platform for
504 understanding the molecular fundamentals of extreme IR resistance. These populations have
505 been evolved using a source of IR with a much higher dose rate than that used previously to
506 evolve IR resistance in *E. coli* (72 Gy/min versus 19 Gy/min) (1). Isolates from the prior evolved
507 populations, CB2000 and CB3000 (1, 2) are only moderately more resistant to this form of IR
508 compared to the parent strain. The higher dose rate in the current protocol may account for the
509 relative sensitivity of the strains derived from the earlier evolution trial.

510 There are distinct differences in the mutations which appear in these populations and
511 those that were previously evolved (1, 2). Only a single mutation previously noted to enhance IR
512 resistance, RecA A290S (1), appears in the four new populations. While enhanced DNA repair is
513 a hallmark of the previously evolved populations and the populations presented here, it appears
514 as though the enhancements are indeed different. In addition, the frequency of transversion
515 mutations detected in the new populations (~50% of all mutations) is far higher than that
516 observed in the earlier studies (~20% of all mutations) (1, 55). This appears to be due to the
517 extreme amount of detected GC to TA transitions, specifically. This transition is a hallmark of A
518 mispairing with template-strand 8-oxodG (56), indicating that DNA damage may be more
519 extreme in cells exposed to electron beam IR. However, the high energy electrons and gamma
520 rays produce similar levels of killing (Fig. 1). A more likely explanation lies with the differences
521 in the dose rate applied. In any case, these new *E. coli* lineages are replete with novel
522 mechanisms of experimentally evolved IR resistance.

523 We do not yet have experimentally evolved *E. coli* that can match the natural IR
524 resistance of the bacterium *D. radiodurans*. However, selection is continuing.

525

526 **Materials and methods**

527 **Growth conditions and bacterial strains used in this study**

528 Unless otherwise stated, *E. coli* cultures were grown in Luria-Bertani (LB) broth (85) at
529 37°C with aeration. *E. coli* were plated on 1.5% LB agar medium (85) and incubated at 37°C.
530 Overnight cultures were grown in a volume of 3 mL for 16 to 18 hr. Exponential phase cultures
531 were routinely diluted 1:100 in 10 mL of LB medium in a 50 mL Erlenmeyer flask and were
532 grown at 37°C with shaking at 200 rpm and were harvested at an OD₆₀₀ of 0.2, unless otherwise
533 noted. After growth to an OD₆₀₀ of 0.2, cultures were placed on ice for 10 min to stop growth
534 before being used for assays.

535 Cultures were plated on tetrazolium agar (TA) for growth competition assays when noted
536 (48, 86). The defined rich medium EZ was mixed per manufacturer's specifications and was
537 supplemented with 0.2% glucose or 0.2% glycerol as indicated (Teknova; Hollister, CA). M9
538 minimal medium (supplemented with 0.2% glucose) was used when indicated (85).

539 All strains used for *in vivo* assays in this study are mutants of *E. coli* K-12 derivative
540 MG1655. Genetic manipulations to transfer mutations or delete genes were performed as
541 previously described (87, 88). Strains used in this study are listed in Table 4.

542 **Serial dilutions and CFU/mL determination**

543 All serial dilutions were performed in 1X phosphate-buffered saline (PBS) (for 1 L: 8 g
544 NaCl, 0.2 g KCl, 1.44 g Na₂HPO₄, KH₂PO₄ 0.24 g with 800 mL dH₂O, adjust pH with HCl to
545 7.4, then add remaining 200 mL dH₂O). Unless otherwise stated, serial dilutions were performed
546 with serial 1:10 dilutions of 100 µL of culture or previous dilution into 900 µL 1X PBS. Before
547 transfer to the next dilution tube, samples were vortexed for 2 seconds and mixed by pipetting to
548 ensure mixing. One-hundred µL of appropriate dilutions were aliquoted onto agar plates of the

549 appropriate medium and were spread-plated utilizing an ethanol-sterilized, bent glass rod. For
550 spot plating, 10 μL of each dilution was aliquoted onto agar plates of the appropriate medium
551 and spots were allowed to dry before plates were incubated as in *Growth conditions*.

552 CFU/mL was calculated using the highest CFU count for each strain assayed that
553 remained between 30 and 300 CFU (ex: 250 CFU on a 10^{-4} dilution plate would be used for
554 calculation over 40 CFU on a 10^{-5} dilution plate).

555

556 **TLD dose validation**

557 An independent dose verification was performed with thermoluminescent dosimeters
558 (TLDs). TLDs are passive dosimeters that are small, accurate and well-suited for dose
559 verification in the routinely used 1.5 mL sample vials. For this project, three TLDs were sealed
560 in a small plastic bag, placed into 1.5 mL tubes containing 900 μL dH_2O , were placed
561 horizontally and submerged under 1.3 cm dH_2O , and irradiated as described in ‘Generalized
562 Linac irradiation protocol’. After the vials were irradiated, the TLDs were read out in the
563 University of Wisconsin Medical Radiation Research center (UWMRRC) TLD lab and
564 compared to the calculated dose. Non-irradiated control TLDs were read out simultaneously to
565 account for any background radiation. The TLDs were calibrated with a separate ^{60}Co beam in
566 the University of Wisconsin Accredited Dosimetry Calibration Laboratory (UWADCL), which
567 provides independent National Institute of Standards and Technology (NIST) traceability for the
568 measurements. This serves as an independent check of the ion-chamber based dose calculation
569 method used to determine the beam-on time for this project. The estimated overall uncertainty on
570 the TLD measured values is +/-5% with a coverage factor of $k=1$.

571

572 **Generalized Linac irradiation protocol**

573 Samples were maintained at 4 °C and transported to the University of Wisconsin Medical
574 Radiation Research Center (UWMRRC) Varian 21EX clinical linear accelerator (Linac) facility
575 for irradiation. The total transport time was approximately 15 min to and from the Linac facility.
576 For each irradiation, the Linac was set to deliver a beam of electrons with 6 MeV of energy to
577 uniformly irradiate all samples (a total of 14) at once. To accomplish this, a special high-dose
578 mode called HDTSe⁻ was utilized, which resulted in a dose rate to the samples of approximately
579 72 Gy/min. The sample tubes were placed horizontally and submerged at a depth of 1.3 cm
580 (measured to the center of the tube's volume) in an ice-water filled plastic tank and set to a
581 source-to-surface distance (SSD) of 61.7 cm. A 30 x 30 cm² square field size was set at the Linac
582 console, which gave an effective field size at this SSD of 18.5 x 18.5 cm². This is ample
583 coverage to provide a uniform dose to all of the sample vials. The monitor unit calculations
584 (determination of the amount of time to leave the Linac on) were based on the American
585 Association of Physicists in Medicine (AAPM) Task Group 51 protocol for reference dosimetry
586 (89). This is the standard method for determining dose per monitor unit in water for radiation
587 therapy calculations. Once the dose was determined in the AAPM Task Group 51 reference
588 protocol conditions (SSD = 100 cm and depth = 10 cm), an ion chamber and water-equivalent
589 plastic slabs were used to translate this dose to the specific conditions used in this project

590

591 **Linac photon mode**

592 The Linac is designed to deliver dose with either electron or photon beams. In photon
593 mode, the electron beam first strikes a flattening filter (not present in electron mode) to produce
594 bremsstrahlung photons and also flatten the beam intensity profile. In order to rule out any

595 effective differences between electron and photon modes during irradiations, the sample vials
596 were irradiated with the same dose rates for both modes by altering the source-to-surface-
597 distance (SSD) for each mode.

598

599 **Ionizing radiation resistance assay using the Linac**

600 Strains were grown in biological triplicate overnight and to an OD₆₀₀ of approximately
601 0.2 in LB as routinely performed. A 1 mL sample for each dose tested (including 0 Gy) was
602 removed and aliquoted into a sterile 1.5 mL microfuge tube. Samples were pelleted by
603 centrifugation at 13 xg for 1 min, and the supernatant was poured off. Samples were resuspended
604 in 1 mL ice-cold 1X phosphate-buffered saline (PBS), and pelleting was repeated. This process
605 was repeated three more times to wash cells. A 100 μ L aliquot of each culture was removed,
606 serial diluted 1:10 in 900 μ L of PBS to a final 10,000-fold dilution and 100 μ L was plated on LB
607 agar to determine the colony forming units (CFU)/mL before irradiation. Samples were
608 maintained at 4 °C and irradiated with the appropriate doses as described. A 100 μ L aliquot of
609 each culture was removed and plated to determine CFU/mL and percent survival as described.

610

611 **Directed evolution protocol using Linac**

612 For each round of directed evolution, separate aliquots of 2 mL of LB medium was
613 inoculated with frozen stock of each population from the previous round of selection. These were
614 incubated overnight with aeration at 37 °C and were grown with usual practices in LB medium
615 to an OD₆₀₀ of 0.2 the next day. Each culture was incubated on ice for 10 minutes to stop growth.
616 Three 1 mL samples were removed and aliquoted into sterile 1.5 mL microfuge tubes. Samples
617 were washed three times with 1 mL ice-cold 1X phosphate-buffered saline (PBS) and

618 resuspended in a final volume of 1 mL of 1X PBS. A 100 μ L aliquot of each culture was
619 removed, serial diluted 1:10 in 900 μ L of PBS to a final 10,000-fold dilution and 100 μ L was
620 plated on LB agar to determine the colony forming units (CFU)/mL before irradiation. Samples
621 were maintained at 4 °C and taken to a Varian 21EX clinical linear accelerator (Linac) for
622 irradiation.

623 After irradiation, an aliquot of each culture was removed, serial diluted 1:10 in 900 μ L of
624 PBS to a final 1,000-fold dilution, and 100 μ L of each serial dilution was plated on LB agar for
625 each dose to determine the CFU/mL after irradiation. LB agar plates were incubated overnight at
626 37 °C. Remaining irradiated cultures pelleted by centrifugation at 13 xg and supernatant was
627 discarded. These pellets were resuspended in 1 mL of fresh LB medium, and this was added to 1
628 mL LB medium in a 5 mL glass culture tube. These resuspensions were incubated overnight with
629 aeration at 37 °C. The following day, the percent survival for each dose was calculated using
630 CFU/mL calculations before and after irradiation at each dose. The overnight culture of each
631 population replicate showing closest to 1% survival was stored at -80 °C and used for the next
632 cycle of selection. One cycle of selection was performed weekly due to limited access to the
633 Linac.

634 The initiating round of selection was done as described above, except the original culture
635 used was an overnight culture of MG1655 prepared from an isolated colony. This protocol was
636 adapted from a previously used protocol (1).

637

638 **UV Resistance Assay**

639 Cells from a single colony of each strain were cultured overnight and then grown to an
640 OD₆₀₀ of ~ 0.2 as in *Growth conditions*. Samples were diluted and spotted onto 25 mL 1.5% LB

641 agar described in the *Serial dilutions*. Spots were dried before the plate lid was removed and
642 spots were exposed to the appropriate dose of UV irradiation using a Spectrolinker XL-1000 UV
643 Crosslinker (Spectronics Corporation, Westbury, NY). Plates were imaged after incubation for 24
644 hr.

645

646 **Resistance to DNA-damaging agents**

647 Cells were grown overnight and to an OD₆₀₀ of approximately 0.2 in LB as routinely
648 performed. Samples were mixed by vortexing for 5 s and were serial diluted 1:10 in 900 µl
649 phosphate-buffered saline (PBS) to a final 100,000-fold dilution. Ten µl was removed from
650 each dilution and spotted onto 30mL 1.5% LB agar medium supplemented with 10 or 7.5 ng/ml
651 ciprofloxacin hydrochloride as specified, 0.5 µM bleomycin, 4 µg/mL mitomycin C, or 5 mM
652 hydroxyurea. Spots were dried before being incubated overnight at 37 °C. Plates were imaged
653 after 48 hr for ciprofloxacin and bleomycin plates.

654

655 **Growth Competition Assay**

656 This assay was adapted from a previously published protocol (2, 48) . To differentiate
657 strains within the competition, a fitness-neutral deletion of the *araBAD* operon was introduced
658 into one of the two strains. This deletion results in red colonies on tetrazolium arabinose (TA)
659 agar plates (48). Briefly, overnight culture of each strain to be competed were mixed 1:1, or 1:9
660 (for growth competitions using isolates from the evolved populations after round 50 of selection
661 or RpoB or ArcB mutations, in favor of the losing competitor) in a 1.5 mL tube. Samples were
662 mixed by vortexing for 5 s and were serial diluted 1:10 in 900 µl phosphate-buffered saline
663 (PBS) to a final dilution of 1:100,000. One hundred uL of the final dilution was spread plated

664 onto TA agar plates to assay for CFU. Seventy μ l of the remaining cell mixture was used to
665 inoculate 5 mL of fresh LB media for growth overnight. This overnight culture was used to
666 inoculate fresh media the following day, and 100 μ l was serially diluted and plated as noted
667 above. This procedure was repeated twice more over a period of two days. The number of white
668 versus red CFU was noted after each day of the competition and the total percentage of the
669 culture for each competitor was determined.

670

671 **Deep Sequencing**

672 Genomic DNA was prepped from overnight cultures prepared from frozen stocks of
673 populations from every even round of selection using the Wizard Genomic DNA Purification Kit
674 (Promega, Madison, WI). DNA samples were submitted to the Department of Energy Joint
675 Genome Institute (Walnut Creek, CA) for sequencing and analysis. DNA was randomly sheared
676 into ~500bp fragments and the resulting fragments were used to create an Illumina library. This
677 library was sequenced on Illumina HiSeq generating 100bp paired end reads. Reads were aligned
678 to the reference genome using BWA (90), downsampled to an average depth of 250 fold
679 coverage with picard (<http://broadinstitute.github.io/picard>) and putative mutations and small
680 indels were called using callvariants.sh from BBMap (sourceforge.net/projects/bbmap).

681 Sequencing results are reported in their entirety in Supplemental Data 1 through 4.
682 However, for analysis of numbers and types of mutations in each population (and consequently
683 for generating Fig. 8, and Table 1 through 3), mutations in genes with high homology throughout
684 the genome (as in *rrs*, *rpl*, *rrn*, *rhs*, and *ins* genes) were not considered due to increased
685 likelihood of a false-positive mutation call. In addition, mutations with inconsistent frequency

686 calls (ex: jumping from 0, to 100, to 0% allele frequency) were also not used. All mutations
687 removed from consideration are also listed in Supplemental Data 1 through 4.

688

689 **Growth Curves**

690 Strains were cultured described as in *Growth conditions* overnight and to an OD₆₀₀ of 0.2
691 in LB medium, EZ medium supplemented with 0.2% glucose (Teknova; Hollister, CA) and M9
692 minimal medium (85) supplemented with 0.2% glucose. Cultures were then diluted 1:100 in the
693 appropriate medium in a clear, flat bottom 96-well plate (Fisher product #: 07-200-656) and
694 incubated overnight in a Biotek Synergy 2 plate reader (Biotek; Winooski, VT) at 37 °C with
695 shaking, with OD₆₀₀ readings taken by the plate reader every 10 minutes.

696

697 **Acknowledgements**

698 This work was supported by grant GM112757 from the National Institute of General Medical
699 Sciences (NIGMS), and by grants 2817 and 502930 from the Joint Genome Institute, United
700 States Department of Energy. Steven Bruckbauer was supported by a Morgridge Biotechnology
701 Scholarship from the Vice Chancellor's Office for Research and Graduate Education, University
702 of Wisconsin-Madison. Joseph Trimarco was supported by the Hilldale Undergraduate
703 Fellowship (UW – Madison).

704

References

706 1. Harris DR, Pollock SV, Wood EA, Goiffon RJ, Klingele AJ, Cabot EL, Schackwitz W,
707 Martin J, Eggington J, Durfee TJ, Middle CM, Norton JE, Popelars M, Li H, Klugman
708 SA, Hamilton LL, Bane LB, Pennacchio L, Albert TJ, Perna NT, Cox MM, Battista JR.

- 709 2009. Directed evolution of radiation resistance in *Escherichia coli*. J Bacteriol
710 191:5240-5252.
- 711 2. Byrne RT, Klingele AJ, Cabot EL, Schackwitz WS, Martin JA, Martin J, Wang Z, Wood
712 EA, Pennacchio C, Pennacchio LA, Perna NT, Battista JR, Cox MM. 2014. Evolution of
713 extreme resistance to ionizing radiation via genetic adaptation of DNA repair. eLife
714 3:e01322.
- 715 3. Daly MJ. 2012. Death by protein damage in irradiated cells. DNA Repair 11:12-21.
- 716 4. Cox MM, Battista JR. 2005. *Deinococcus radiodurans* - The consummate survivor. Nat
717 Rev Microbiol 3:882-892.
- 718 5. Tanaka M, Earl AM, Howell HA, Park MJ, Eisen JA, Peterson SN, Battista JR. 2004.
719 Analysis of *Deinococcus radiodurans*'s transcriptional response to ionizing radiation and
720 desiccation reveals novel proteins that contribute to extreme radioresistance. Genetics
721 168:21-33.
- 722 6. Fredrickson JK, Li SM, Gaidamakova EK, Matrosova VY, Zhai M, Sulloway HM,
723 Scholten JC, Brown MG, Balkwill DL, Daly MJ. 2008. Protein oxidation: key to bacterial
724 desiccation resistance? Isme J 2:393-403.
- 725 7. Battista JR, Earl AM, Park MJ. 1999. Why is *Deinococcus radiodurans* so resistant to
726 ionizing radiation? Trends Microbiol 7:362-5.
- 727 8. Rainey FA, Ray K, Ferreira M, Gatz BZ, Nobre MF, Bagaley D, Rash BA, Park MJ, Earl
728 AM, Shank NC, Small AM, Henk MC, Battista JR, Kampfer P, da Costa MS. 2005.
729 Extensive diversity of ionizing-radiation-resistant bacteria recovered from Sonoran desert
730 soil and description of nine new species of the genus *Deinococcus* obtained from a single
731 soil sample. Appl Environ Microbiology 71:5225-5235.

- 732 9. Rainey FA, Nobre MF, Schumann P, Stackebrandt E, Dacosta MS. 1997. Phylogenetic
733 diversity of the *Deinococci* as determined by 16s ribosomal DNA sequence comparison.
734 Int J Syst Bacteriol 47:510-514.
- 735 10. Daly MJ, Gaidamakova EK, Matrosova VY, Kiang JG, Fukumoto R, Lee DY, Wehr NB,
736 Viteri GA, Berlett BS, Levine RL. 2010. Small-molecule antioxidant proteome-shields in
737 *Deinococcus radiodurans*. PLoS One 5:e12570.
- 738 11. Daly MJ, Gaidamakova EK, Matrosova VY, Vasilenko A, Zhai M, Venkateswaran A,
739 Hess M, Omelchenko MV, Kostandarithes HM, Makarova KS, Wackett LP, Fredrickson
740 JK, Ghosal D. 2004. Accumulation of Mn(II) in, *Deinococcus radiodurans* facilitates
741 gamma-radiation resistance. Science 306:1025-1028.
- 742 12. Slade D, Radman M. 2011. Oxidative Stress Resistance in *Deinococcus radiodurans*.
743 Microbiol Mol Biol Rev 75:133-191.
- 744 13. Selvam K, Duncan JR, Tanaka M, Battista JR. 2013. DdrA, DdrD, and PprA:
745 components of UV and mitomycin C resistance in *Deinococcus radiodurans* R1. PLoS
746 One 8:e69007.
- 747 14. Earl AM, Mohundro MM, Mian IS, Battista JR. 2002. The IrrE protein of *Deinococcus*
748 *radiodurans* R1 is a novel regulator of *recA* expression. J Bacteriol 184:6216-24.
- 749 15. Harris DR, Tanaka M, Saveliev SV, Jolivet E, Earl AM, Cox MM, Battista JR. 2004.
750 Preserving genome integrity: The DdrA protein of *Deinococcus radiodurans* R1. PLoS
751 Biol 2:e304.
- 752 16. Witkin EM. 1946. Inherited differences in sensitivity to radiation in *Escherichia coli*.
753 Proc Natl Acad Sci USA 32:59-68.

- 754 17. Parisi A, Antoine AD. 1974. Increased radiation resistance of vegetative *Bacillus*
755 *pumilus*. Appl Microbiol 28:41-6.
- 756 18. Davies R, Sinskey AJ. 1973. Radiation-resistant mutants of *Salmonella typhimurium*
757 LT2: development and characterization. J Bacteriol 113:133-44.
- 758 19. Erdman IE, Thatcher FS, Macqueen KF. 1961. Studies on the irradiation of
759 microorganisms in relation to food preservation. II. Irradiation resistant mutants. Can J
760 Microbiol 7:207-15.
- 761 20. Chou HH, Chiu HC, Delaney NF, Segre D, Marx CJ. 2011. Diminishing returns epistasis
762 among beneficial mutations decelerates adaptation. Science 332:1190-1192.
- 763 21. Cooper TF, Rozen DE, Lenski RE. 2003. Parallel changes in gene expression after
764 20,000 generations of evolution in *Escherichia coli*. Proc Natl Acad Sci USA 100:1072-
765 1077.
- 766 22. Good BH, McDonald MJ, Barrick JE, Lenski RE, Desai MM. 2017. The dynamics of
767 molecular evolution over 60,000 generations. Nature 551:45-50.
- 768 23. Lieberman TD, Michel JB, Aingaran M, Potter-Bynoe G, Roux D, Davis MR, Skurnik D,
769 Leiby N, LiPuma JJ, Goldberg JB, McAdam AJ, Priebe GP, Kishony R. 2011. Parallel
770 bacterial evolution within multiple patients identifies candidate pathogenicity genes. Nat
771 Genet 43:1275-1280.
- 772 24. Tenaille O, Barrick JE, Ribick N, Deatherage DE, Blanchard JL, Dasgupta A, Wu GC,
773 Wielgoss S, Cruveiller S, Medigue C, Schneider D, Lenski RE. 2016. Tempo and mode
774 of genome evolution in a 50,000-generation experiment. Nature 536:165-170.

- 775 25. Wannier TM, Kunjapur AM, Rice DP, McDonald MJ, Desai MM, Church GM. 2018.
776 Adaptive evolution of genomically recoded *Escherichia coli*. Proc Natl Acad Sci USA
777 115:3090-3095.
- 778 26. Woods R, Schneider D, Winkworth CL, Riley MA, Lenski RE. 2006. Tests of parallel
779 molecular evolution in a long-term experiment with *Escherichia coli*. Proc Natl Acad Sci
780 USA 103:9107-9112.
- 781 27. Luksza M, Lassig M. 2014. A predictive fitness model for influenza. Nature 507:57-61.
- 782 28. Miller CR, Joyce P, Wichman HA. 2011. Mutational effects and population dynamics
783 during viral adaptation challenge current models. Genetics 187:185-202.
- 784 29. Miller CR, Nagel AC, Scott L, Settles M, Joyce P, Wichman HA. 2016. Love the one
785 you're with: replicate viral adaptations converge on the same phenotypic change. PeerJ
786 4:e2227.
- 787 30. Morris DH, Gostic KM, Pompei S, Bedford T, Luksza M, Neher RA, Grenfell BT, Lassig
788 M, McCauley JW. 2018. Predictive modeling of influenza shows the promise of applied
789 evolutionary biology. Trends Microbiol 26:102-118.
- 790 31. Zanini F, Brodin J, Thebo L, Lanz C, Bratt G, Albert J, Neher RA. 2015. Population
791 genomics of inpatient HIV-1 evolution. eLife 4:e11282.
- 792 32. Kvitek DJ, Sherlock G. 2013. Whole genome, whole population sequencing reveals that
793 loss of signaling networks is the major adaptive strategy in a constant environment. PLoS
794 Genet 9:e1003972.
- 795 33. Lang GI, Rice DP, Hickman MJ, Sodergren E, Weinstock GM, Botstein D, Desai MM.
796 2013. Pervasive genetic hitchhiking and clonal interference in forty evolving yeast
797 populations. Nature 500:571-574.

- 798 34. Alexandrov LB, Nik-Zainal S, Wedge DC, Aparicio S, Behjati S, Biankin AV, Bignell
799 GR, Bolli N, Borg A, Borresen-Dale AL, Boyault S, Burkhardt B, Butler AP, Caldas C,
800 Davies HR, Desmedt C, Eils R, Eyfjord JE, Foekens JA, Greaves M, Hosoda F, Hutter B,
801 Ilicic T, Imbeaud S, Imielinski M, Jager N, Jones DTW, Jones D, Knappskog S, Kool M,
802 Lakhani SR, Lopez-Otin C, Martin S, Munshi NC, Nakamura H, Northcott PA, Pajic M,
803 Papaemmanuil E, Paradiso A, Pearson JV, Puente XS, Raine K, Ramakrishna M,
804 Richardson AL, Richter J, Rosenstiel P, Schlesner M, Schumacher TN, Span PN, Teague
805 JW, Totoki Y., Tutt A. N. J., Valdes-Mas, R., van Buuren, M. M., van 't Veer, L.,
806 Vincent-Salomon, A., Waddell, N., Yates, L. R., Zucman-Rossi, J., Futreal, P. A.,
807 McDermott, U., Lichter, P., Meyerson, M., Grimmond, S. M., Siebert, R., Campo, E.,
808 Shibata, T., Pfister, S. M., Campbell, P. J., Stratton, M. R., Australian Pancreatic Canc,
809 Genome, IcgC Breast Canc Consortium, IcgC Mmml- Seq Consortium, IcgC PedBrain.
810 2013. Signatures of mutational processes in human cancer. *Nature* 500:415-421.
- 811 35. Alexandrov LB, Jones PH, Wedge DC, Sale JE, Campbell PJ, Nik-Zainal S, Stratton MR.
812 2015. Clock-like mutational processes in human somatic cells. *Nat Genet* 47:1402-1407.
- 813 36. Alexandrov LB, Ju YS, Haase K, Van Loo P, Martincorena I, Nik-Zainal S, Totoki Y,
814 Fujimoto A, Nakagawa H, Shibata T, Campbell PJ, Vineis P, Phillips DH, Stratton MR.
815 2016. Mutational signatures associated with tobacco smoking in human cancer. *Science*
816 354:618-622.
- 817 37. Bolli N, Avet-Loiseau H, Wedge DC, Van Loo P, Alexandrov LB, Martincorena I,
818 Dawson KJ, Iorio F, Nik-Zainal S, Bignell GR, Hinton JW, Li YL, Tubio JMC, McLaren
819 S, Meara SO, Butler AP, Teague JW, Mudie L, Anderson E, Rashid N, Tai YT, Shammas
820 MA, Sperling AS, Fulciniti M, Richardson PG, Parmigiani G, Magrangeas F, Minvielle

821 S, Moreau P, Attal M, Facon T, Futreal PA, Anderson KC, Campbell PJ, Munshi NC.
822 2014. Heterogeneity of genomic evolution and mutational profiles in multiple myeloma.
823 Nat Commun 5:2997.

824 38. Gundem G, Van Loo P, Kremeyer B, Alexandrov LB, Tubio JMC, Papaemmanuil E,
825 Brewer DS, Kallio HML, Hoegnas G, Annala M, Kivinummi K, Goody V, Latimer C,
826 O'Meara S, Dawson KJ, Isaacs W, Emmert-Buck MR, Nykter M, Foster C, Kote-Jarai Z,
827 Easton D, Whitaker HC, Neal DE, Cooper CS, Eeles RA, Visakorpi T, Campbell PJ,
828 McDermott U, Wedge DC, Bova GS, Grp IPU. 2015. The evolutionary history of lethal
829 metastatic prostate cancer. Nature 520:353-357.

830 39. Hunter KW, Amin R, Deasy S, Ha NH, Wakefield L. 2018. Genetic insights into the
831 morass of metastatic heterogeneity. Nat Rev Cancer 18:211-223.

832 40. Kandoth C, McLellan MD, Vandin F, Ye K, Niu BF, Lu C, Xie MC, Zhang QY,
833 McMichael JF, Wyczalkowski MA, Leiserson MDM, Miller CA, Welch JS, Walter MJ,
834 Wendl MC, Ley TJ, Wilson RK, Raphael BJ, Ding L. 2013. Mutational landscape and
835 significance across 12 major cancer types. Nature 502:333-339.

836 41. Martincorena I, Campbell PJ. 2015. Somatic mutation in cancer and normal cells. Science
837 349:1483-1489.

838 42. Morganella S, Alexandrov LB, Glodzik D, Zou XQ, Davies H, Staaf J, Sieuwerts AM,
839 Brinkman AB, Martin S, Ramakrishna M, Butler A, Kim HY, Borg A, Sotiriou C, Futreal
840 PA, Campbell PJ, Span PN, Van Laere S, Lakhani SR, Eyfjord JE, Thompson AM,
841 Stunnenberg HG, de Vijver MJV, Martens JWM, Borresen-Dale AL, Richardson AL,
842 Kong G, Thomas G, Sale J, Rada C, Stratton MR, Birney E, Nik-Zainal S. 2016. The
843 topography of mutational processes in breast cancer genomes. Nature Commun 7:11383.

- 844 43. Nik-Zainal S, Van Loo P, Wedge DC, Alexandrov LB, Greenman CD, Lau KW, Raine
845 K, Jones D, Marshall J, Ramakrishna M, Shlien A, Cooke SL, Hinton J, Menzies A,
846 Stebbings LA, Leroy C, Jia MM, Rance R, Mudie LJ, Gamble SJ, Stephens PJ, McLaren
847 S, Tarpey PS, Papaemmanuil E, Davies HR, Varela I, McBride DJ, Bignell GR, Leung K,
848 Butler AP, Teague JW, Martin S, Jonsson G, Mariani O, Boyault S, Miron P, Fatima A,
849 Langerod A, Aparicio S, Tutt A, Sieuwerts AM, Borg A, Thomas G, Salomon AV,
850 Richardson AL, Borresen-Dale AL, Futreal PA, Stratton MR, Campbell PJ, Int Canc
851 Genome C. 2012. The life history of 21 breast cancers. *Cell* 149:994-1007.
- 852 44. Vogelstein B, Papadopoulos N, Velculescu VE, Zhou SB, Diaz LA, Kinzler KW. 2013.
853 Cancer genome landscapes. *Science* 339:1546-1558.
- 854 45. Wedge DC, Gundem G, Mitchell T, Woodcock DJ, Martincorena I, Ghori M, Zamora J,
855 Butler A, Whitaker H, Kote-Jarai Z, Alexandrov LB, Van Loo P, Massie CE, Dentre S,
856 Warren AY, Verrill C, Berney DM, Dennis N, Merson S, Hawkins S, Howat W, Lu YJ,
857 Lambert A, Kay J, Kremeyer B, Karaszi K, Luxton H, Camacho N, Marsden L, Edwards
858 S, Matthews L, Bo V, Leongamornlert D, McLaren S, Ng A, Yu YW, Zhang HW,
859 Dadaev T, Thomas S, Easton DF, Ahmed M, Bancroft E, Fisher C, Livni N, Nicol D,
860 Tavare S, Gill P, Greenman C, Khoo V, Van As N, Kumar, P., Ogden, C., Cahill, D.,
861 Thompson, A., Mayer, E., Rowe, E., Dudderidge, T., Gnanapragasam, V., Shah, N. C.,
862 Raine, K., Jones, D., Menzies, A., Stebbings, L., Teague, J., Hazell, S., Corbishley, C., de
863 Bono, J., Attard, G., Isaacs, W., Visakorpi, T., Fraser, M., Boutros, P. C., Bristow, R. G.,
864 Workman, P., Sander, C., Hamdy, F. C., Futreal, A., McDermott, U., Al-Lazikani, B.,
865 Lynch, A. G., Bova, G. S., Foster, C. S., Brewer, D. S., Neal, D. E., Cooper, C. S., Eeles,
866 R. A., Camcap Study Grp, Tcga Consortium. 2018. Sequencing of prostate cancers

- 867 identifies new cancer genes, routes of progression and drug targets. Nat Genet 50:682-
868 692.
- 869 46. Rokyta DR, Joyce P, Caudle SB, Miller C, Beisel CJ, Wichman HA. 2011. Epistasis
870 between beneficial mutations and the phenotype-to-fitness map for a ssDNA virus. PLoS
871 Genet 7:e1002075.
- 872 47. Bruckbauer ST, Trimarco JD, Henry C, Wood EA, Battista JR, Cox MM. 2019. A variant
873 of the *Escherichia coli* anaerobic transcription factor FNR exhibiting diminished
874 promoter activation function enhances ionizing radiation resistance. PLoS One in press.
- 875 48. Lenski RE, Rose MR, Simpson SC, Tadler SC. 1991. Long-term experimental evolution
876 in *Escherichia-coli*.1. Adaptation and divergence during 2,000 generations. American
877 Naturalist 138:1315-1341.
- 878 49. Povirk LF. 1987. Mutational specificity of bleomycin. Proc Amer Assoc Cancer Res
879 28:117-117.
- 880 50. Povirk LF. 1987. Bleomycin-induced base substitutions in the lambda-cI gene. Environ
881 Mutagen 9:86-86.
- 882 51. Hendricks SP, Mathews CK. 1998. Differential effects of hydroxyurea upon
883 deoxyribonucleoside triphosphate pools, analyzed with vaccinia virus ribonucleotide
884 reductase. J Biol Chem 273:29519-29523.
- 885 52. Sakano K, Oikawa S, Hasegawa K, Kawanishi S. 2001. Hydroxyurea induces site-
886 specific DNA damage via formation of hydrogen peroxide and nitric oxide. Jap J Cancer
887 Res 92:1166-1174.
- 888 53. Singh A, Xu YJ. 2016. The cell killing mechanisms of hydroxyurea. Genes 7:99.

- 889 54. Weinberger M, Trabold PA, Lu M, Sharma K, Huberman JA, Burhans WC. 1999.
890 Induction by adozelesin and hydroxyurea of origin recognition complex-dependent DNA
891 damage and DNA replication checkpoints in *Saccharomyces cerevisiae*. J Biol Chem
892 274:35975-35984.
- 893 55. Xie C-X, Xu A, Wu L-J, Yao J-M, Yang J-B, Yu Z-L. 2004. Comparison of base
894 substitutions in response to nitrogen ion implantation and ⁶⁰Co-gamma ray irradiation in
895 *Escherichia coli*. Genet Mol Biol 27:284-290.
- 896 56. Wang D, Kreutzer DA, Essigmann JM. 1998. Mutagenicity and repair of oxidative DNA
897 damage: insights from studies using defined lesions. Mut Res-Fund Mol Mech Mutagen
898 400:99-115.
- 899 57. Elena SF, Lenski RE. 2003. Evolution experiments with microorganisms: The dynamics
900 and genetic bases of adaptation. Nature Rev Genet 4:457-469.
- 901 58. Toprak E, Veres A, Michel JB, Chait R, Hartl DL, Kishony R. 2012. Evolutionary paths
902 to antibiotic resistance under dynamically sustained drug selection. Nature Genet 44:101-
903 U140.
- 904 59. Amundsen SK, Taylor AF, Chaudhury AM, Smith GR. 1986. recD: the gene for an
905 essential third subunit of exonuclease V. Proc Natl Acad Sci USA 83:5558-62.
- 906 60. Biek DP, Cohen SN. 1986. Identification and characterization of *recD*, a gene affecting
907 plasmid maintenance and recombination in *Escherichia coli*. J Bacteriol 167:594-603.
- 908 61. Chaudhury AM, Smith GR. 1984. A new class of *Escherichia coli* *recBC* mutants -
909 implications for the role of RecBC enzyme in homologous recombination. Proc Natl
910 Acad Sci USA 81:7850-7854.

- 911 62. Thaler DS, Sampson E, Siddiqi I, Rosenberg SM, Thomason LC, Stahl FW, Stahl MM.
912 1989. Recombination of bacteriophage lambda in recD mutants of *Escherichia coli*.
913 Genome 31:53-67.
- 914 63. Uranga LA, Reyes ED, Patidar PL, Redman LN, Lusetti SL. 2017. The cohesin-like
915 RecN protein stimulates RecA-mediated recombinational repair of DNA double-strand
916 breaks. Nature Commun 8:15282.
- 917 64. Wang G, Maier RJ. 2008. Critical role of RecN in recombinational DNA repair and
918 survival of *Helicobacter pylori*. Infect Immun 76:153-160.
- 919 65. Picksley SM, Morton SJ, Lloyd RG. 1985. The *recN* locus of *Escherichia coli* K12:
920 molecular analysis and identification of the gene product. Mol Gen Genet 201:301-7.
- 921 66. Meddows TR, Savory AP, Grove JJ, Moore T, Lloyd RG. 2005. RecN protein and
922 transcription factor DksA combine to promote faithful recombinational repair of DNA
923 double-strand breaks. Mol Microbiol 57:97-110.
- 924 67. Brena-Valle M, Serment-Guerrero J. 1998. SOS induction by gamma-radiation in
925 *Escherichia coli* strains defective in repair and/or recombination mechanisms. Mutagen
926 13:637-641.
- 927 68. Cashel M, Gentry DR, Hernandez VJ, Vinella D. 1996. The Stringent Response, p 1458-
928 1495. In Neidhardt FC, Curtiss RI (ed), *Escherichia coli* and *Salmonella*: Cell Mol Biol,
929 vol 1. ASM Press, Washington, D. C.
- 930 69. Trautinger BW, Lloyd RG. 2002. Modulation of DNA repair by mutations flanking the
931 DNA channel through RNA polymerase. EMBO J 21:6944-6953.
- 932 70. McGlynn P, Lloyd RG. 2000. Modulation of RNA polymerase by (p)ppGpp reveals a
933 RecG-dependent mechanism for replication fork progression. Cell 101:35-45.

- 934 71. Epshtein V, Kamarthapu V, McGary K, Svetlov V, Ueberheide B, Proshkin S, Mironov
935 A, Nudler E. 2014. UvrD facilitates DNA repair by pulling RNA polymerase backwards.
936 Nature 505:372-377.
- 937 72. Landick R, Stewart J, Lee DN. 1990. Amino acid changes in conserved regions of the
938 beta subunit of *Escherichia coli* RNA polymerase alter transcription pausing and
939 termination. Genes Develop4:1623-1636.
- 940 73. Barrick JE, Kauth MR, Strelisoff CC, Lenski RE. 2010. *Escherichia coli* rpoB Mutants
941 Have Increased Evolvability in Proportion to Their Fitness Defects. Mol Biol Evol
942 27:1338-1347.
- 943 74. Severinov K, Soushko M, Goldfarb A, Nikiforov V. 1993. Rifampicin region revisited -
944 new rifampicin-resistant and streptolydigin-resistant mutants in the beta subunit of
945 *Escherichia coli* RNA polymerase. J Biol Chem 268:14820-14825.
- 946 75. Zhou YN, Lubkowska L, Hui M, Court C, Chen S, Court DL, Strathern J, Jin DJ,
947 Kashlev M. 2013. Isolation and characterization of RNA Polymerase *rpoB* mutations that
948 alter transcription slippage during elongation in *Escherichia coli*. J Biol Chem 288:2700-
949 2710.
- 950 76. Deatherage DE, Kepner JL, Bennett AF, Lenski RE, Barrick JE. 2017. Specificity of
951 genome evolution in experimental populations of *Escherichia coli* evolved at different
952 temperatures. Proc Natl Acad Sci USA 114:E1904-E1912.
- 953 77. Tenaille O, Rodriguez-Verdugo A, Gaut RL, McDonald P, Bennett AF, Long AD, Gaut
954 BS. 2012. The molecular diversity of adaptive convergence. Science 335:457-461.
- 955 78. Avrani S, Bolotin E, Katz S, Hershberg R. 2017. Rapid genetic adaptation during the first
956 four months of survival under resource exhaustion. Mol Biol Evol 34:1758-1769.

- 957 79. Conrad TM, Frazier M, Joyce AR, Cho BK, Knight EM, Lewis NE, Landick R, Palsson
958 BO. 2010. RNA polymerase mutants found through adaptive evolution reprogram
959 *Escherichia coli* for optimal growth in minimal media. Proc Natl Acad Sci USA
960 107:20500-20505.
- 961 80. Harden MM, He A, Creamer K, Clark MW, Hamdallah I, Martinez KA, Kresslein RL,
962 Bush SP, Slonczewski JL. 2015. Acid-adapted strains of *Escherichia coli* K-12 obtained
963 by experimental evolution. Appl Environ Microbiol 81:1932-1941.
- 964 81. He A, Penix SR, Basting PJ, Griffith JM, Creamer KE, Camperchioli D, Clark MW,
965 Gonzales AS, Erazo JSC, George NS, Bhagwat AA, Slonczewski JL. 2017. Acid
966 evolution of *Escherichia coli* K-12 eliminates amino acid decarboxylases and reregulates
967 catabolism. Appl Environ Microbiol 83:UNSP e00442-17.
- 968 82. Mehta P, Casjens S, Krishnaswamy S. 2004. Analysis of the lambdoid prophage element
969 e14 in the *E. coli* K-12 genome. BMC Microbiol 4:4.
- 970 83. Charusanti P, Conrad TM, Knight EM, Venkataraman K, Fong NL, Xie B, Gao YA,
971 Palsson BO. 2010. Genetic basis of growth adaptation of *Escherichia coli* after deletion
972 of *pgi*, a major metabolic gene. PLoS Genet 6:e1001186.
- 973 84. Wang X, Kim Y, Ma Q, Hong SH, Pokusaeva K, Sturino JM, Wood TK. 2010. Cryptic
974 prophages help bacteria cope with adverse environments. Nat Commun 1:147.
- 975 85. Miller JH. 1992. A Short Course in Bacterial Genetics: A Laboratory Manual and
976 Handbook for *Escherichia coli* and Related Bacteria. Cold Spring Harbor Laboratory,
977 Cold Spring Harbor, NY.
- 978 86. Lenski RE. 1991. Quantifying fitness and gene stability in microorganisms. Biotech
979 15:173-92.

- 980 87. Warming S, Costantino N, Court DL, Jenkins NA, Copeland NG. 2005. Simple and
981 highly efficient BAC recombineering using galK selection. *Nuc Acids Res* 33:e36.
- 982 88. Datsenko KA, Wanner BL. 2000. One-step inactivation of chromosomal genes in
983 *Escherichia coli* K-12 using PCR products. *Proc Natl Acad Sci USA* 97:6640-6645.
- 984 89. Almond PR, Biggs PJ, Coursey BM, Hanson WF, Huq MS, Nath R, Rogers DWO. 1999.
985 AAPM's TG-51 protocol for clinical reference dosimetry of high-energy photon and
986 electron beams. *Med Phys* 26:1847-1870.
- 987 90. Li H, Durbin R. 2009. Fast and accurate short read alignment with Burrows-Wheeler
988 transform. *Bioinform* 25:1754-1760.
- 989
- 990

991 **Figure Legends**

992 **Fig. 1. Cell killing with electron beam versus photon beam ionizing radiation.** Early
993 exponential phase cultures of MG1655 were exposed to electron beam or photon beam IR as
994 described in the Materials and Methods. Percent survival was determined via CFU/mL counts
995 pre- and post-irradiation. Results are representative of a single experiment performed in
996 biological triplicate.

997

998 **Fig. 2. Directed evolution scheme and lineage nomenclature. (A) Scheme.** Briefly, overnight
999 cultures were grown from a freezer stock of the parent strain/the evolved population from the
1000 previous round of selection. This overnight culture was used to inoculate fresh LB rich medium
1001 and cultures were grown to early exponential phase. These cultures were then separated into
1002 multiple aliquots and washed 3X in 1X PBS to remove LB medium. One aliquot of each
1003 population was irradiated with the same dose that killed 99% of the population in the previous
1004 round of selection, and the remaining aliquots were irradiated with higher doses. A portion of the
1005 irradiated aliquots were plated to determine percent survival, while the remaining culture was
1006 resuspended in fresh LB medium. These were then grown overnight, and the culture that was
1007 nearest to 1% survival (as determined by CFU counts from pre- and post-irradiation cultures)
1008 was stored at -80° C. One round of selection was conducted weekly due to limited access to the
1009 Linac. **(B) Nomenclature.** We have generated four lineages of highly IR-resistant *E. coli*,
1010 designated IR9, IR10, IR11, and IR12. A designated round of selection indicates a population at
1011 that round (Ex: IR9-50 is lineage IR9 after 50 rounds of selection). Each population has been
1012 stored at -80 °C as a ‘fossil record’ of evolution. Clonal isolates generated by streak plating a

1013 population then streak plating ten separate isolated colonies are designated by a numeral value
1014 added to the parent population nomenclature (Ex: The first isolate from IR9-50 is IR9-50-1).

1015

1016 **Fig. 3. Documentation of increased IR resistance.** (A) *Increase in dose required to kill 99% of*
1017 *cells.* Each data point indicates the dose of IR that each population was given prior to being
1018 outgrown overnight (Step 6 in Fig. 2) and stored at -80° C. (Step 7 in Fig. 2). The percent
1019 survival was estimated from a single replicate at each round of selection. (B) *Survival curves of*
1020 *evolved populations compared to previously evolved Escherichia coli isolates and Deinococcus*
1021 *radiodurans.* Early exponential phase cultures of the indicated strains were exposed to electron
1022 beam IR as described in the Materials and Methods. CB2000 and CB3000 are isolates from *E.*
1023 *coli* populations evolved to withstand γ -ray IR (1, 2). Error bars represent the standard deviation
1024 of CFU/mL calculations from a single experiment performed in biological triplicate.

1025

1026 **Fig. 4. Growth curves of evolved isolates in rich and minimal medium.** (A) *Growth curves of*
1027 *isolates in LB rich medium.* (B) *Growth curves of isolates in EZ defined rich medium*
1028 *supplemented with 0.2% glucose.* (C) *Growth curves of isolates in M9 defined minimal medium*
1029 *supplemented with 0.2% glucose.* Cultures of indicated strains were grown in the appropriate
1030 medium overnight and then to early exponential phase as described in the Materials and
1031 Methods. All cultures were incubated at 37 °C during growth. Early exponential phase cultures
1032 were diluted 1:100 in the appropriate medium, and then incubated overnight in a Biotek Synergy
1033 2 plate reader, with OD₆₀₀ measurements taken automatically every 5 minutes. Each growth
1034 curve is a representative replicate from an experiment performed in biological triplicate.

1035

1036 **Fig. 5. Growth competitions of evolved isolates.** (A) *Growth competition of IR9-50-1 against*
1037 *Founder $\Delta e14$.* (B) *Growth competition of IR10-50-1 against Founder $\Delta e14$.* (C) *Growth*
1038 *competition of IR11-50-1 against Founder $\Delta e14$.* (D) *Growth competition of IR12-50-1 against*
1039 *Founder $\Delta e14$.* Growth competitions were performed as described in the Materials and Methods.
1040 Briefly, competitions were started with an excess of the evolved isolate so that competitions
1041 could be carried out to 72 hr (at approximately a 9:1 ratio of evolved isolate to Founder $\Delta e14$).
1042 Even with an excess of IR9-50-1, this isolate was outcompeted by 48 hr. Deleting the *araBAD*
1043 operon causes a red colony phenotype with no fitness cost that allows for differentiation of the
1044 two strains in competition on TA medium. IR11-50-1 is red on TA medium without alteration of
1045 the *araBAD* operon, so this competition was performed against Founder $\Delta e14$ *araBAD*⁺. Error
1046 bars represent the standard deviation of CFU/mL calculations of an experiment performed in
1047 biological triplicate. Results shown are representative of two independent experiments.

1048

1049 **Fig. 6. Evolved isolates exhibit variable survival of UV irradiation.** Five isolates from each
1050 population were grown in LB medium overnight and then to early exponential phase as described
1051 in the Materials and Methods. Cultures were serial diluted in 1X PBS, and then 10 μ L of each
1052 dilution was spot plated onto LB agar. Once spots dried, plates were exposed to UV irradiation
1053 and were then incubated overnight before imaging. Results shown are representative of two
1054 independent experiments performed.

1055

1056 **Fig. 7. Evolved isolates exhibit variable survival of various DNA damaging agents.** Five
1057 isolates from each population were grown in LB medium overnight and then to early exponential
1058 phase as described in the Materials and Methods. Cultures were serial diluted in 1X PBS, and

1059 then 10 μ L of each dilution was spot plated onto LB agar with the indicated DNA-damaging
1060 agent. Once spots dried the plates were then incubated overnight before imaging. Results shown
1061 are representative of two independent experiments performed.

1062

1063 **Fig. 8. Mutations in evolving populations. (A-D)** *Allele frequencies as a function of selection*
1064 *round.* Panels A-D reflect the indicated population, IR9, IR10, IR11, and IR12, respectively.
1065 Whole populations at each even round of selection were deep-sequenced by the Joint Genome
1066 Institute (JGI) as described in the *Materials and Methods*. Every mutation that reached at least
1067 2% frequency at some point in a single population are depicted as single lines. The sole black
1068 line in each graph represents the loss of the ϵ 14 prophage. Mutations that reach a frequency of
1069 “1.00” are fixed, and subsequent mutations occur within that genetic background. The y-axis
1070 represents the allele frequency of each single mutation within the population (i.e. a mutation at
1071 0.5 is in 50% of the isolates in the population). The x-axis represents the round of selection.
1072 Allele frequency data was generated from every even cycle of selection. Graphs were generated
1073 using the R library “ggplot2”. Line colors are utilized primarily to allow ready distinctions
1074 between subpopulations, but otherwise have no significance. Data used to generate these plots
1075 are contained within Supplemental Data 1 through 4. **(E)** *Number of mutations over rounds of*
1076 *selection in evolving populations.* Each data point represents the total number of detected
1077 mutations at or above 2% frequency in each sequenced whole population. The number of
1078 mutations generally increases, but experience dips as major sub-populations are driven to
1079 extinction. Data used to generate this plot are contained within Supplemental Data 1 through 4.

1080

1081 **Fig. 9. Mutations which contribute to IR resistance in the evolved isolate IR9-50-1. (A)** *IR*
1082 *resistance of Founder Δe14 derivatives containing mutations from lineage IR9.* Mutations were
1083 moved singly or in combination from IR9-50-1 (in the case of ArcB N405D, from IR9-20-1; the
1084 *recD* deletion was made in the Founder Δe14 parent strain) into the Founder Δe14 strain
1085 background as described in the Materials and Methods. A '+' symbol indicates that the variant is
1086 present in that strain. **(B)** *IR resistance of IR9-50-1 derivatives containing reversions of*
1087 *mutations to the wild-type sequence.* Wild-type sequences of the gene encoding the indicated
1088 protein variants was moved from Founder Δe14 into IR9-50-1 as described in the Materials and
1089 Methods (IR9-50-1 does not have a ArcB variant, therefore no reversion was tested in this
1090 strain). A '-' symbol indicates that the variant was reverted to the wild-type allele in that strain.
1091 Each strain was assayed for IR resistance alongside biological triplicate of the parent strain (a
1092 Founder Δe14 or IR9-50-1 control) and the average percent survival of the experimental strains
1093 was compared to that of the parent strain. All strains were exposed to 1000 Gy of electron beam
1094 IR and percent survival was determined via calculating CFU/mL before and after irradiation.
1095 Error bars represent the standard deviation of CFU/mL calculations of at least two independent
1096 experiments performed in biological triplicate. Statistical significance of percent survival relative
1097 to the parent strain was determined using a two-tailed Student's T-test. The '**' and '****'
1098 represent p-values of < 0.05 and < 0.001, respectively.

1099

1100 **Fig. 10. Frequencies of mutations implicated in IR resistance over rounds of selection.**
1101 Frequencies of mutations in genes implicated in evolved IR resistance (*rpoB*, *recA*, *recD*, *recN*)
1102 and the loss of the e14 prophage are depicted. Both synonymous and non-synonymous mutations
1103 are included. These data seemingly indicate two separate paths to acquiring IR resistance: loss of

1104 the e14 prophage, gain of an *rpoB*, then *recD*, then *recN* mutation, in that order (IR9, IR11,
1105 IR12), or gain of a *recA* and *recD* mutation in concert (IR10). In lineages IR11 and IR12, these
1106 two pathways to IR resistance appear in direct competition, with the *rpoB*, *recD*, and *recN* path
1107 being the apparent ‘winner’. Data used to generate these plots are contained within Supplemental
1108 Data 1 through 4.

1109

1110 **Fig. 11. Effects of prevalent mutations on growth.** Two mutations from lineage IR9 have
1111 opposite effects on growth; ArcB N405D greatly enhances growth of Founder Δ e14 whereas the
1112 RpoB S72N/RpoC K1172I mutations greatly hinder growth. These results suggest that mutation
1113 not seen to affect IR resistance (ArcB N405D) may be selected for in these populations to
1114 counteract the deleterious growth effects of mutations which enhance IR resistance. Growth
1115 competition assays were performed as described in the Materials and Methods. Initial ratios of
1116 each strain were purposefully mixed at 9 (loser):1 (winner) so that growth competition assays
1117 could be carried out for longer than 24 hr. Results shown are representative of two independent
1118 experiments performed.

1119

1120

1121

1122

1123

1124

1125

1126

1127 **Tables**

1128

1129 **Table 1. Number and types of mutations in evolved populations after 50 cycles of selection.**

1130 Mutations in coding regions that likely cause loss of function of the protein product (single and
1131 double base insertions/deletions, gain or loss of stop codons, and loss of start codons) appeared
1132 in each population. However, IR9-50 had the most predicted loss of function mutations (72)
1133 compared to the other three populations (IR10-50: 48, IR11-50: 40, IR12-50: 49). Of these
1134 mutations in all populations, -1 frameshift mutations were the most common, followed by
1135 introduced stop codons.

1136

1137 **Table 2. Mutations that are likely candidates for enhancing IR resistance.** Proteins listed are

1138 encoded by genes that have i) mutations that were non-synonymous; ii) mutations that occurred
1139 in a gene that was mutated in at least two additional populations; iii) mutations that achieved at
1140 least 10% abundance at some point during selection in each population in which they appeared;
1141 and iv) the mutation remained in the population at round 50 of selection. The mutations in RecA
1142 and Nth were included as these are the only proteins with the same variant present in two
1143 populations. The bolded variants are fixed in the indicated population, the variants listed in black
1144 are present above 2% frequency at round 50 of selection, and variants listed in gray were present
1145 in the indicated lineage but have been driven extinct by round 50 of selection.

1146

1147 **Table 3. Number of mutations in isolates from evolved populations after 50 cycles of**

1148 **selection.** Nomenclature of the isolates indicates the lineage (ex: IR9) and round of selection
1149 (ex:50) from which the isolate was derived. The remaining numeral distinguishes the individual

1150 isolates.

1151

1152 **Table 4. List of strains used in this study.** Strains generated in this study were constructed as
1153 described in the Materials and Methods. A ‘wt’ designation indicates that the protein is variant at
1154 the indicated allele in the evolved isolate but has been swapped to the wild-type (MG1655)
1155 allele. The ‘*’ symbol indicates that this nucleotide position is in reference to the NCBI
1156 GenBank U00096.3 reference genome.

1157

1158

1159

1160 Table 1

1161

1162

	Parent bp	Mutant bp	IR9-50	IR10-50	IR11-50	IR12-50
Transitions	AT	GC	93	106	94	110
	GC	AT	180	158	130	223
Transversions	AT	CG	26	17	11	25
	GC	TA	154	116	84	143
	AT	TA	81	58	59	85
	GC	CG	41	25	31	51
Transitions			273	264	224	333
Transversions			302	216	185	304
Total			575	480	409	637
Coding	Synonymous		127	124	98	171
	Non-synonymous		340	275	237	363
	dN/dS		2.68	2.22	2.42	2.12
	Stop gained		29	15	12	16
	Stop lost		1	2	0	1
	Start lost		0	0	1	2
	Insertions	+1	1	2	2	3
		+2	0	0	0	0
		+3	0	0	1	0
		+12	0	0	1	0
	Deletions	-1	40	26	21	26
		-2	0	1	1	2
		-3	1	0	0	0
Non-coding	SNPs		81	70	65	92
	Insertions	+1	0	0	0	0
		+2	0	0	0	1
		+3	0	0	0	0
	Deletions	-1	3	6	4	6
		-2	0	0	0	1
-3		0	0	0	0	
Allele frequencies	Fixed (>99%)		107	84	20	76
	>50%		242	109	130	150
	>10 %		309	199	205	320
	>2%		620	515	439	676

1163 Table 2

1164

1165

Pathway	Protein	IR9	IR10	IR11	IR12
Anaerobic respiration	ArcB	N405D	D166Y S280R L90 fs Y71C	R100H S74W	S24P K547 fs
Copper metabolism	CopA	V270F		T525A	A812V
DNA metabolism	DinI	R28H P14A	W71*	I66N	S26Y
	Nth		C203Y E160K		C203Y K85N
	RecA	Y294C	A290S	A290S E286G	E19K
	RecD	A90E L188* L223* P99*	N124D Q463* L301M	A550E A39G C71 fs G307W W534R	S92I A271E C103* T568A
	RecN	K429Q E271G R118L	F144L	R102P S382R	A361T R285C R368H S310L
RNA polymerase	RpoB	S72N S391P	F15L K1200E	P535L S574F	T600I

1166 Table3

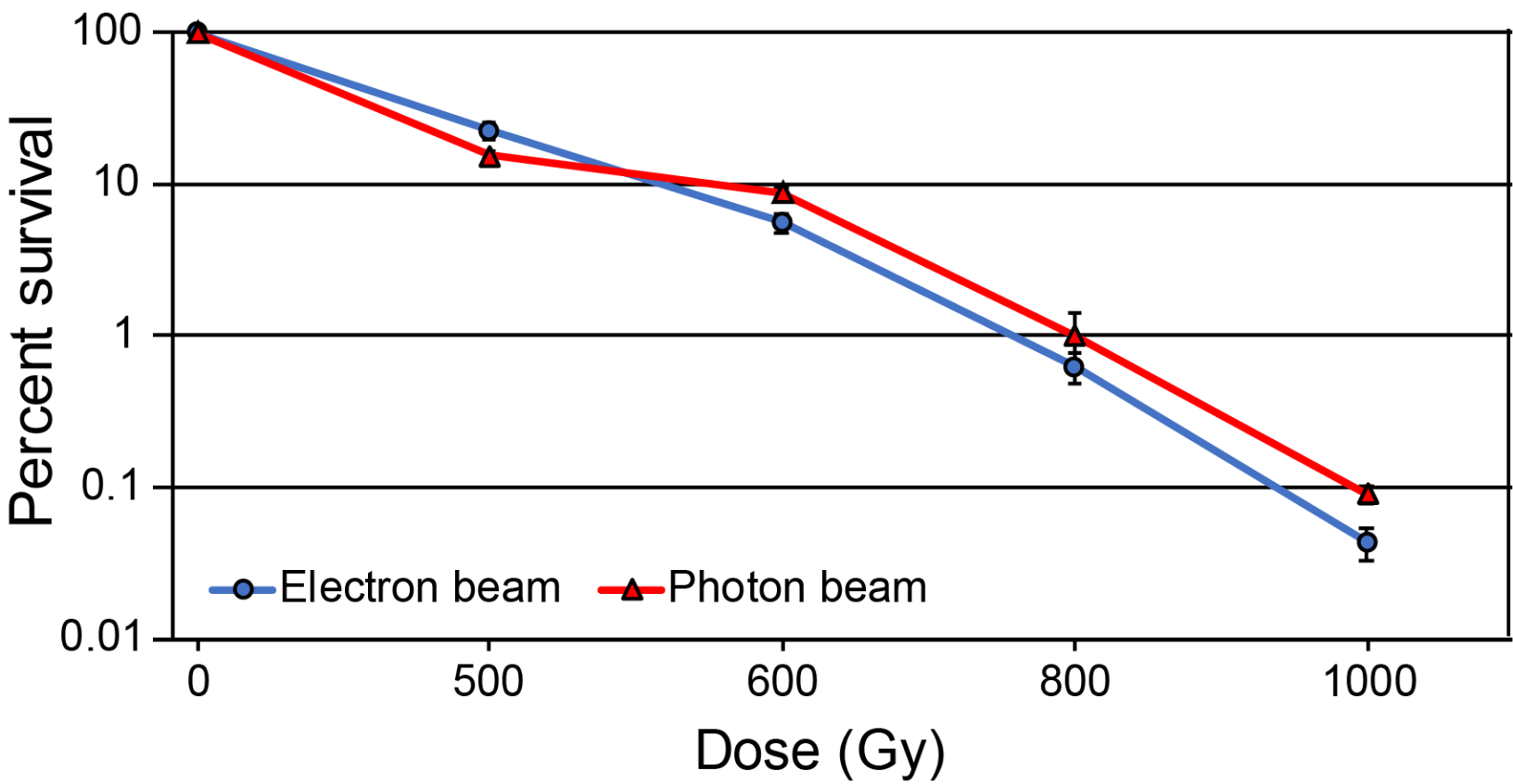
1167

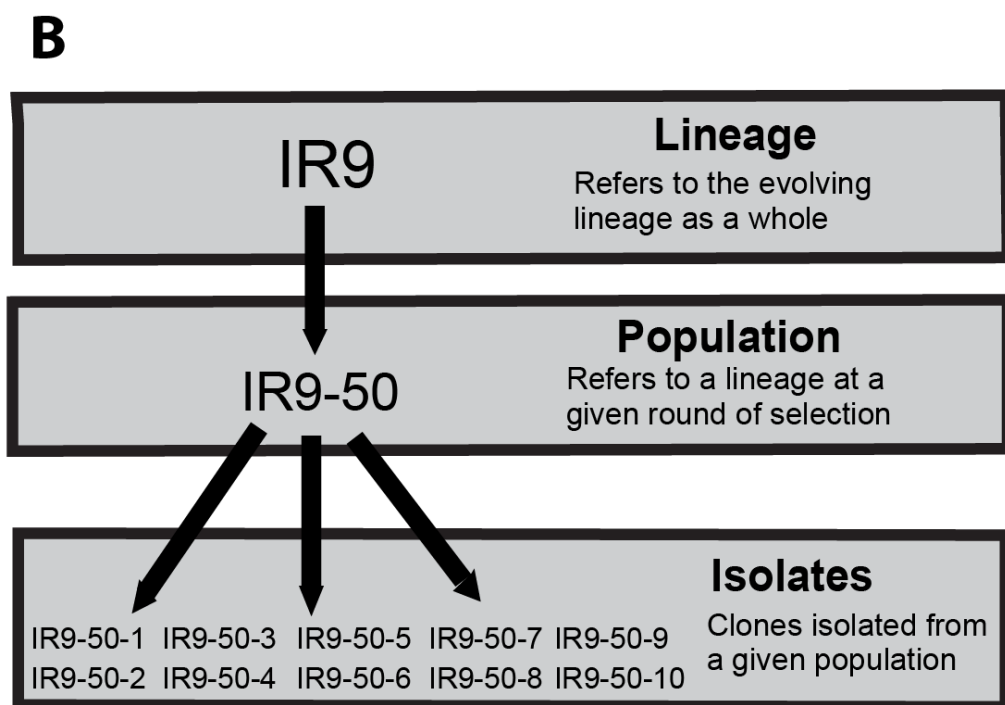
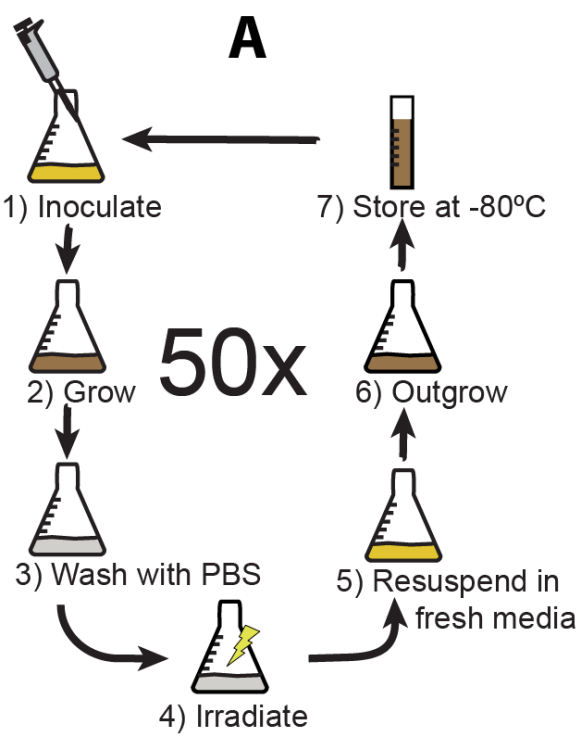
1168

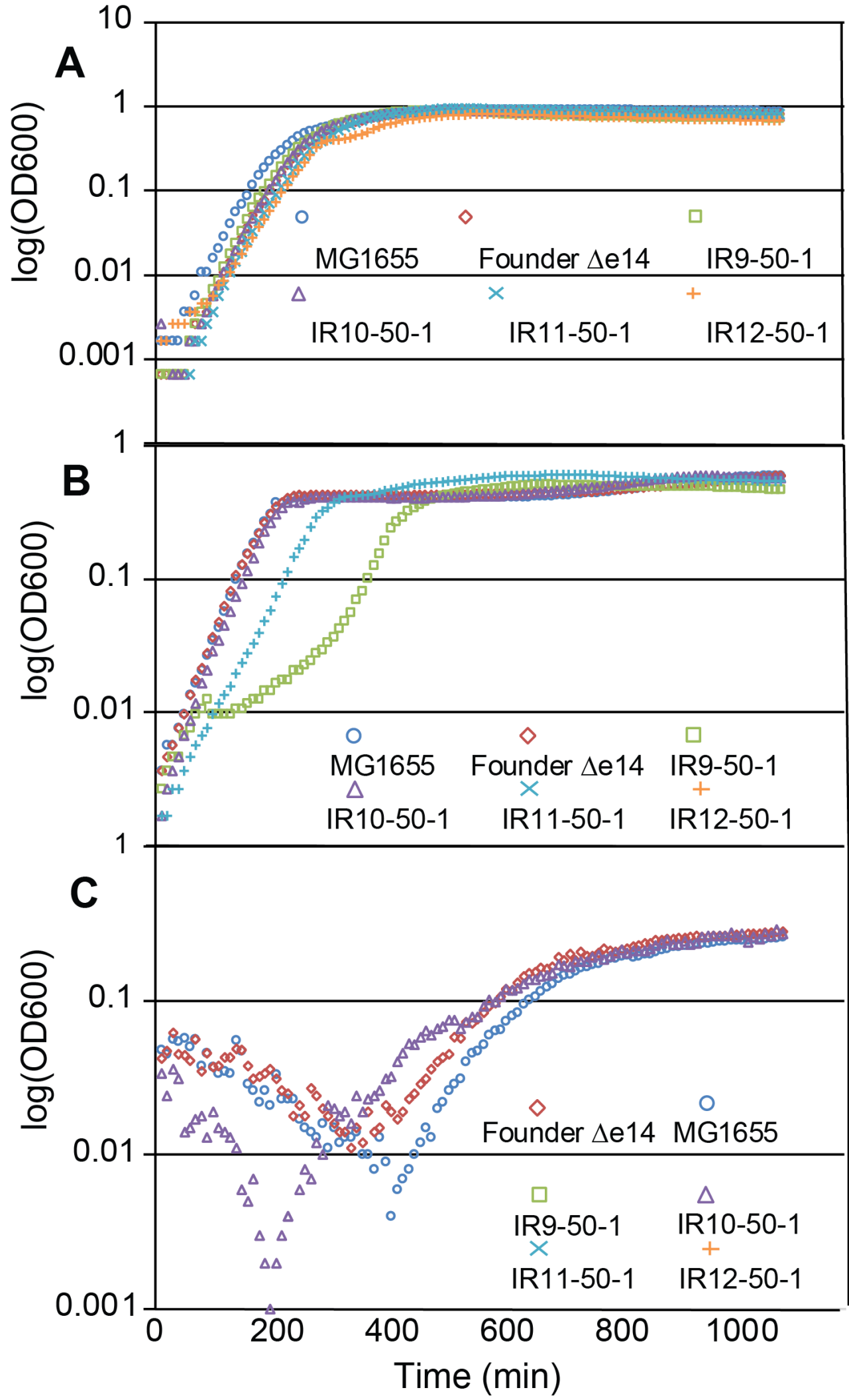
Isolate	Number of Mutations
IR9-50-1	312
IR9-50-2	298
IR9-50-3	299
IR9-50-4	314
IR9-50-5	322
IR10-50-1	184
IR10-50-2	188
IR10-50-3	197
IR10-50-4	210
IR10-50-5	191
IR11-50-1	200
IR11-50-2	192
IR11-50-3	194
IR11-50-4	182
IR11-50-5	197
IR12-50-1	280
IR12-50-2	241
IR12-50-3	245
IR12-50-4	232
IR12-50-5	237

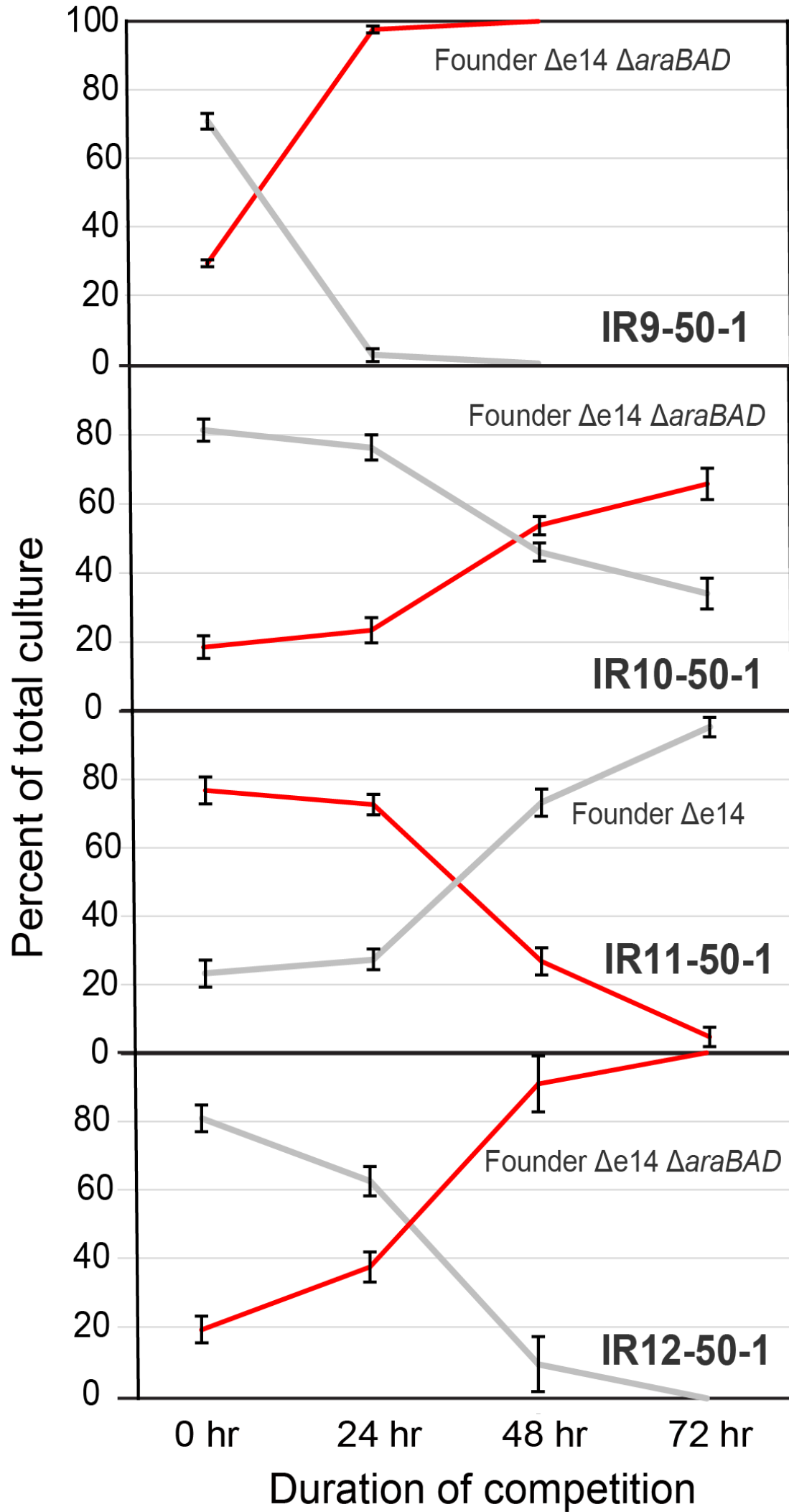
Strain	Relevant Genotype	Source
MG1655	YbhJ L54I + MntP G25D + RIP321 A 4296380* ACG + GlpR C 3560455* CG + GatC ACC 2173360* A	Blattner, 1997
EAW7704 (Founder Δe14)	MG1655 Δe14 + RbsR L92R + CytR Q110 stop + <i>fabI/ycjD</i> int (G 1351174* A) + <i>yifN/ppiC</i> int (T 3959934* C)	Harris, 2009
IR9-50	MG1655 exposed to 50 iterative rounds of IR; mixed population	This study
IR10-50	MG1655 exposed to 50 iterative rounds of IR; mixed population	This study
IR11-50	MG1655 exposed to 50 iterative rounds of IR; mixed population	This study
IR12-50	MG1655 exposed to 50 iterative rounds of IR; mixed population	This study
IR9-50-1	Isolate from IR9-50	This study
IR9-50-2	Isolate from IR9-50	This study
IR9-50-3	Isolate from IR9-50	This study
IR9-50-4	Isolate from IR9-50	This study
IR9-50-5	Isolate from IR9-50	This study
IR10-50-1	Isolate from IR10-50	This study
IR10-50-2	Isolate from IR10-50	This study
IR10-50-3	Isolate from IR10-50	This study
IR10-50-4	Isolate from IR10-50	This study
IR10-50-5	Isolate from IR10-50	This study
IR11-50-1	Isolate from IR11-50	This study
IR11-50-2	Isolate from IR11-50	This study
IR11-50-3	Isolate from IR11-50	This study
IR11-50-4	Isolate from IR11-50	This study
IR11-50-5	Isolate from IR11-50	This study
IR12-50-1	Isolate from IR12-50	This study
IR12-50-2	Isolate from IR12-50	This study
IR12-50-3	Isolate from IR12-50	This study
IR12-50-4	Isolate from IR12-50	This study
IR12-50-5	Isolate from IR12-50	This study
CB2000	Isolate from IR-resistant evolved population IR-2-20	Harris, 2009
CB3000	Isolate from IR-resistant evolved population IR-3-20	Harris, 2009
EAW792	Founder Δe14 + ArcB N405D	This study
EAW971	Founder Δe14 + CopA V270F	This study
EAW766	Founder Δe14 + DinI R28H	This study
JDT56	Founder Δe14 + RecA A290S	This study
EAW726	Founder Δe14 + RecD A90E	This study
EAW725	Founder Δe14 + RecN K429Q	This study
EAW756	Founder Δe14 + RpoB S72N/RpoC K1172I	This study
EAW748	Founder Δe14 + RecD A90E + RecN K428H	This study
EAW904	Founder Δe14 + RecD A90E + RpoB S72N/RpoC K1172I	This study
EAW781	Founder Δe14 + RecD A90E + RecN K428H + RpoB S72N/RpoC K1172I	This study
EAW972	IR9-50-1 + CopA V270 wt	This study
EAW1047	IR9-50-1 + DinI R28 wt	This study
EAW973	IR9-50-1 + RecD A90 wt	This study
EA1024	IR9-50-1 + RecN K429 wt	This study
EAW981	IR9-50-1 + RpoB S72/RpoC K1172 wt	This study
EAW1021	IR9-50-1 + RecD A90 wt + RpoB S72/RpoC K1172 wt	This study
EAW1046	IR9-50-1 + RecD A90 wt + RpoB S72/RpoC K1172 wt + RecN K429 wt	This study
STB75	Founder Δe14 ΔaraBAD	Bruckbauer, 2018

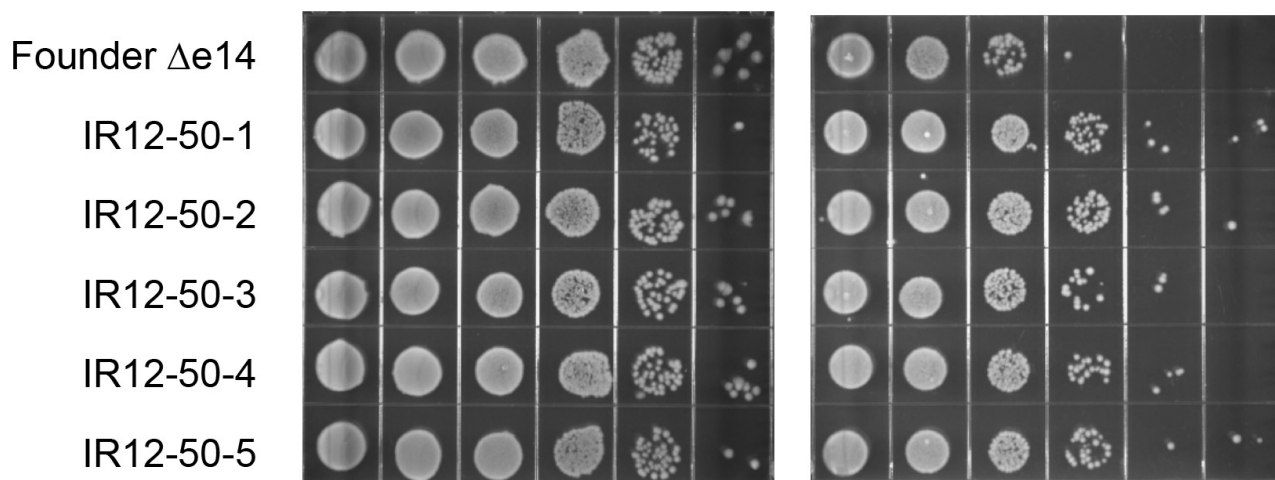
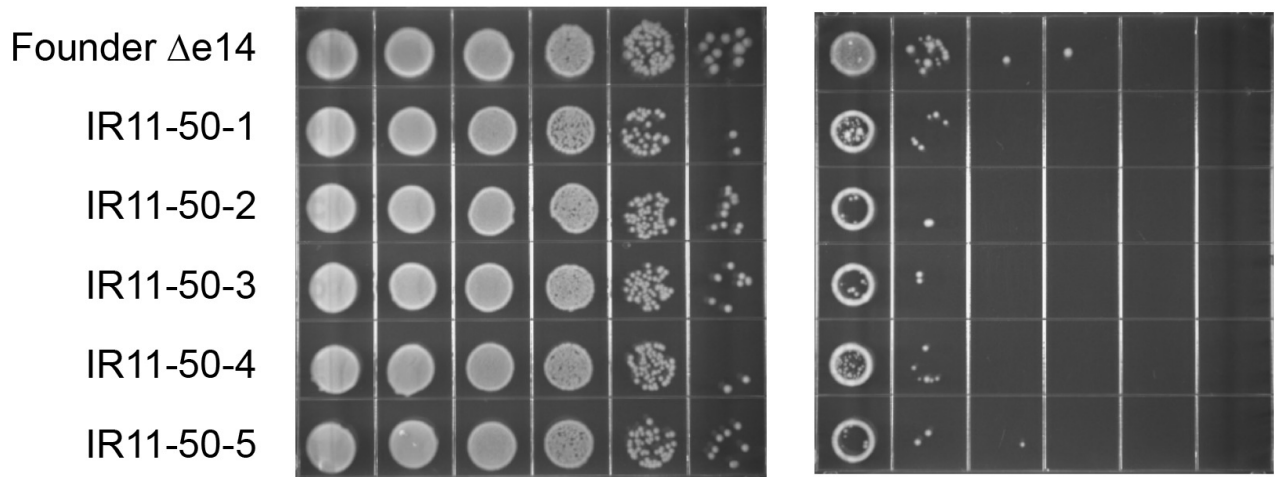
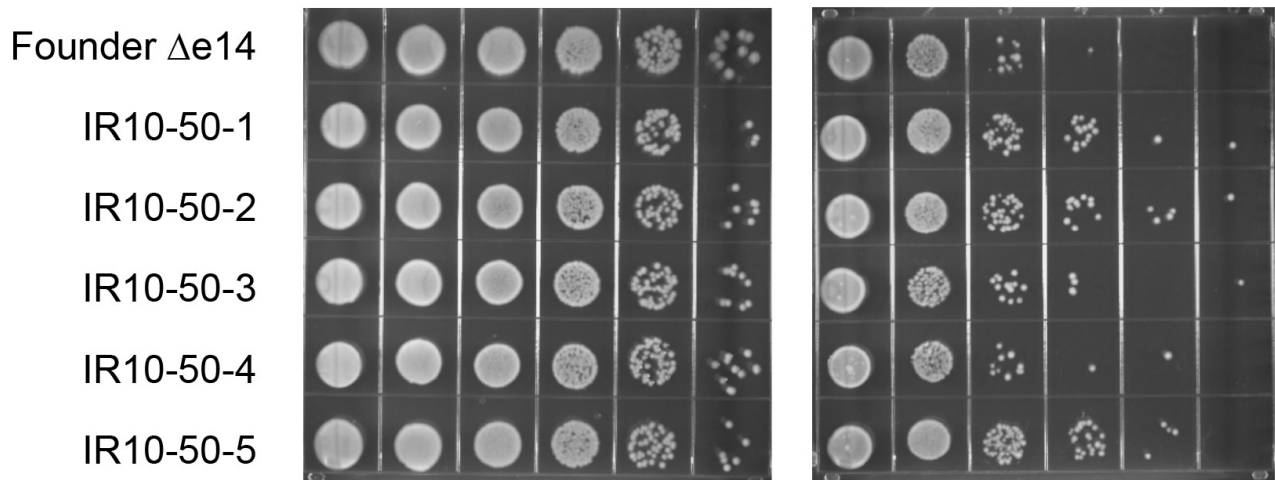
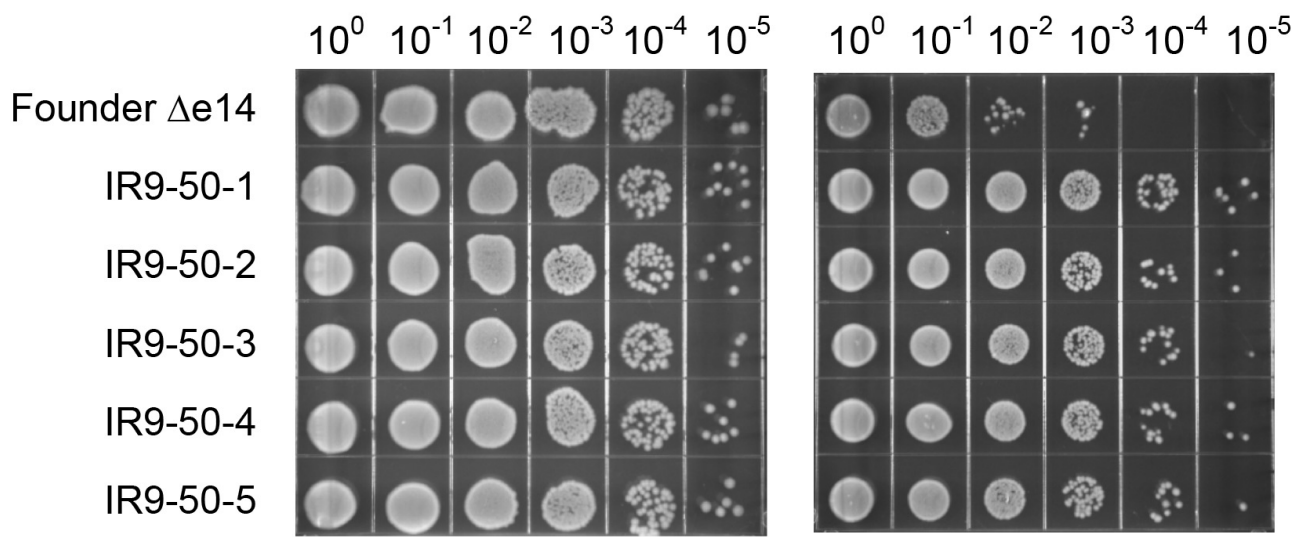
* nucleotide position compared to NCBI GenBank U00096.3 reference sequence





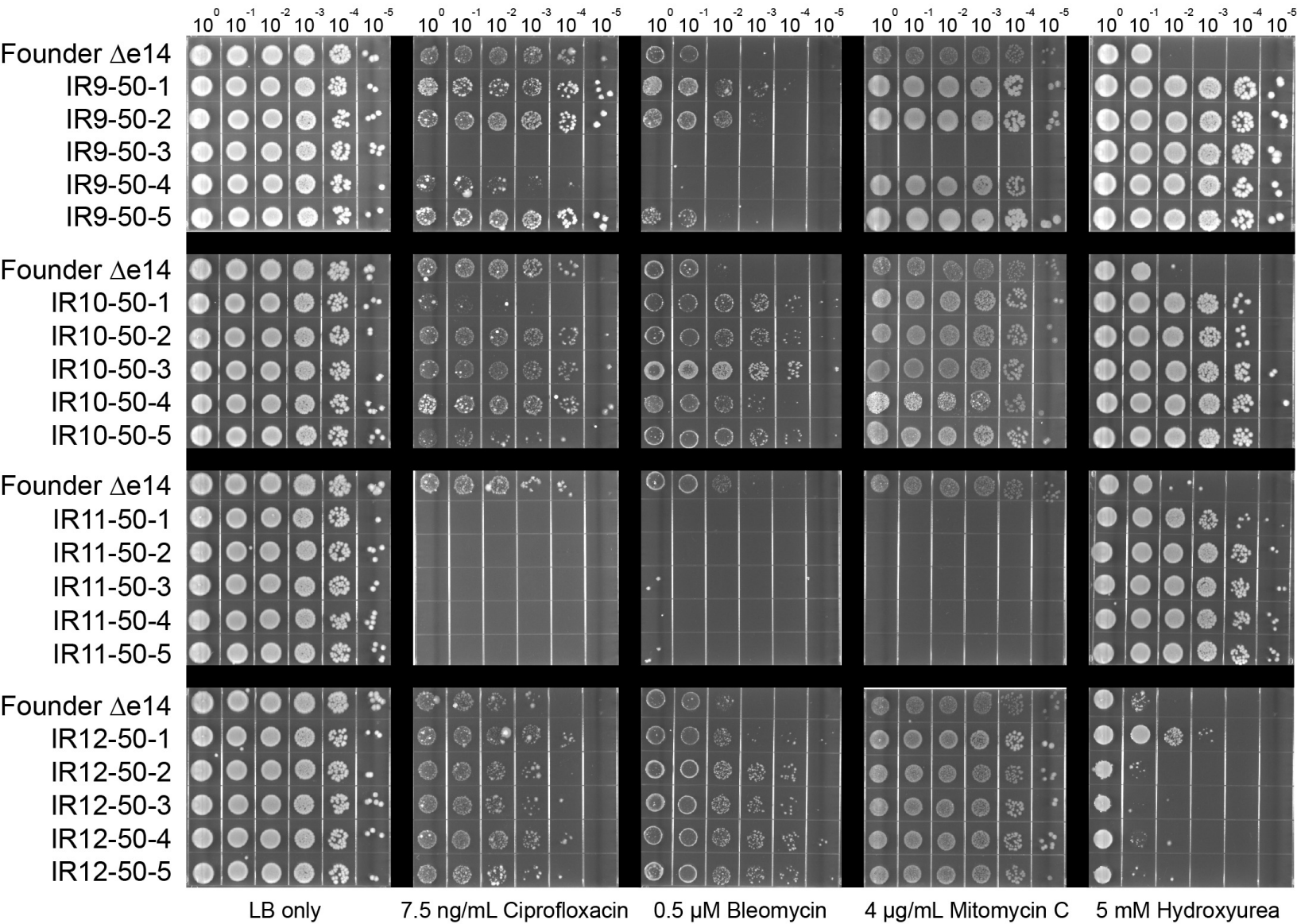


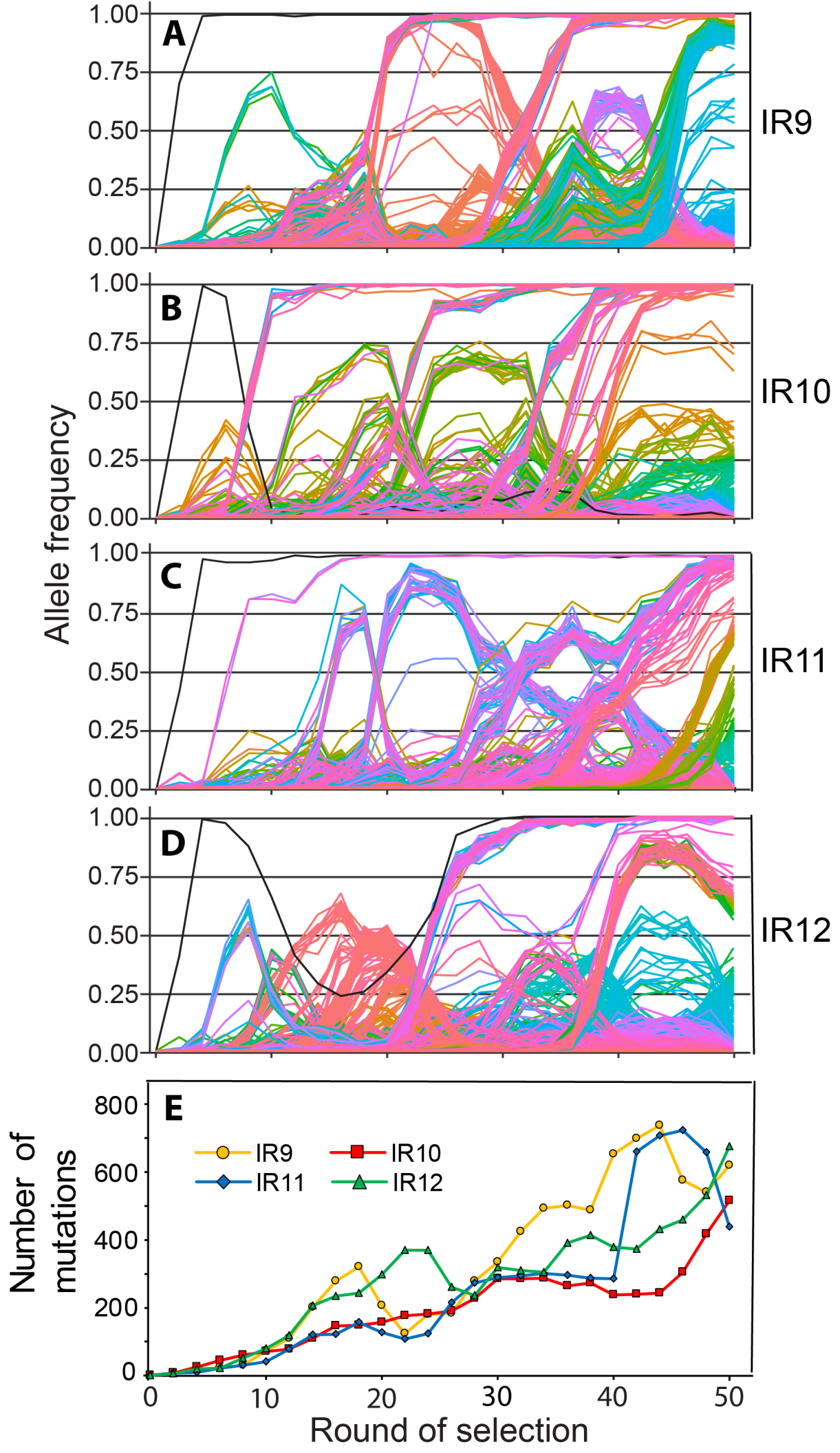


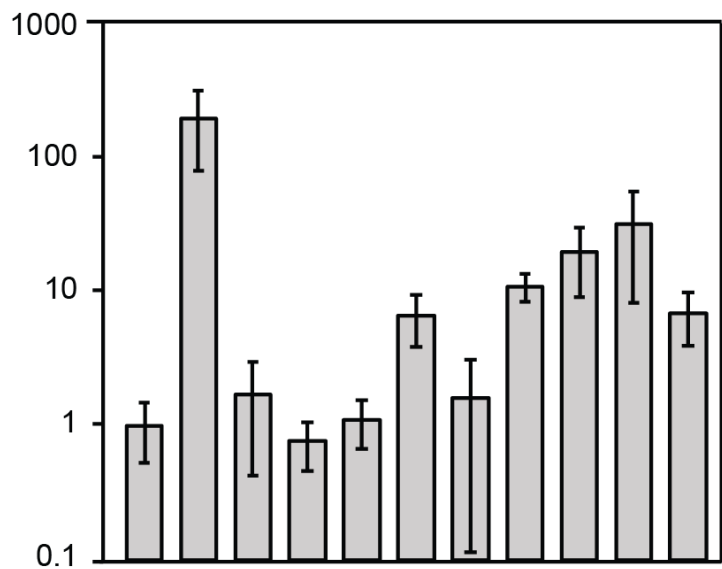


0 J/m²

120 J/m²

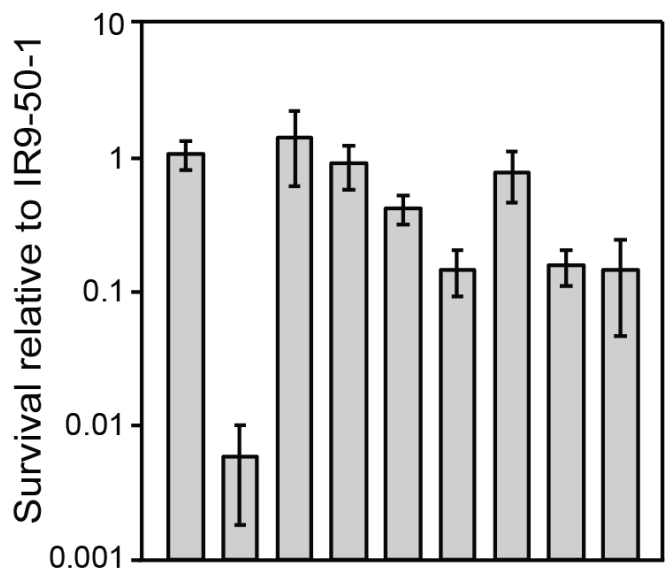




A

Founder $\Delta e14$	IR9-50-1		+						
				+					
					+				
						+		+	Δ
							+		+
								+	+
									+

ArcB N405D
 CopA V270F
 DinI R28H
 RecD A90E
 RecN K426Q
 RpoB S72N/RpoC K1172I

B

IR9-50-1	Founder $\Delta e14$		-					
				-				
					-		-	-
						-		-
							-	-
								-

